bioRxiv preprint first posted online Oct. 22, 2018; doi: http://dx.doi.org/10.1101/449884. The copyright holder for this preprint (which was not peer-reviewed) is the author/funder, who has granted bioRxiv a license to display the preprint in perpetuity. All rights reserved. No reuse allowed without permission.

Trem2 promotes anti-inflammatory responses in microglia and is suppressed under pro-inflammatory conditions

Short running title: TREM2 drives anti-inflammatory processes

Wenfei Liu[1], Orjona Taso[1], Rui Wang[1], Pablo Garcia-Reitboeck[2], William D. Andrews[3], Thomas M. Piers[2], Jennifer M. Pocock[2], Damian M. Cummings[1], John Hardy[4], Frances A. Edwards[1], Dervis A. Salih[1*]

[1]Department of Neuroscience, Physiology and Pharmacology, UCL, Gower Street, London WC1E 6BT, UK

[2]Department of Neuroinflammation, Institute of Neurology, UCL, London WC1N 1PJ, UK

[3]Department of Cell and Developmental Biology, UCL, Gower Street, London WC1E 6BT, UK

[4]Department of Neurodegenerative Diseases, Institute of Neurology, UCL, London WC1N 1PJ, UK

*Correspondence: dervis.salih@ucl.ac.uk

bioRxiv preprint first posted online Oct. 22, 2018; doi: http://dx.doi.org/10.1101/449884. The copyright holder for this preprint (which was not peer-reviewed) is the author/funder, who has granted bioRxiv a license to display the preprint in perpetuity. All rights reserved. No reuse allowed without permission.

Acknowledgements

Thanks to Dr Lion Shahab for statistical advice. WL funded by a UCL PhD Scholarship. DAS and FAE funded by Alzheimer's Research UK. FAE and DMC also funded by the UK Dementia Research Institute. PG-R was supported by a Clinical Research fellowship from Alzheimer's Research UK. TMP was supported by Eisai, working with the Eisai:UCL Therapeutic Innovation Group (TIG) and was also supported by funding to JMP and JH from the Innovative Medicines Initiative 2 Joint Undertaking under grant agreement 115976. The Joint Undertaking receives support from the European Union's Horizon 2020 research and innovation programme and the European Federation of Pharmaceutical Industries and Associations (EFPIA). JH is also supported by the Dolby Foundation.

Word Count:

234 words (Abstract), 15,925 words (Whole Document)

bioRxiv preprint first posted online Oct. 22, 2018; doi: http://dx.doi.org/10.1101/449884. The copyright holder for this preprint (which was not peer-reviewed) is the author/funder, who has granted bioRxiv a license to display the preprint in perpetuity. All rights reserved. No reuse allowed without permission.

Abstract

Recent genome-wide association studies have reported that, amongst other microglial genes, variants in *TREM2* can profoundly increase the incidence of developing Alzheimer's disease (AD). We have investigated the role of TREM2 in primary microglial cultures from wild-type mice by using siRNA to decrease *Trem2* expression, and in parallel from knock-in mice heterozygous or homozygous for the *Trem2* R47H AD risk variant (from the Jackson laboratories). The prevailing phenotype of *Trem2* R47H knock-in mice was decreased expression levels of *Trem2* in microglia, which resulted in decreased density of microglia in the hippocampus. Overall, primary microglia with reduced *Trem2* expression, either by siRNA or from the R47H knock-in mice, displayed a similar phenotype. Comparison of the effects of decreased *Trem2* expression under conditions of LPS pro-inflammatory or IL4 anti-inflammatory stimulation revealed the importance of *Trem2* in driving a number of the genes up-regulated in the anti-inflammatory phenotype, whether treated with RNAi or performed with microglia carrying the R47H variant. In particular, *Trem2* knockdown decreased levels of the transcription factor STAT6. STAT6 is the key mediator downstream from IL4 and controls expression of genes including *Arg1,* which also showed decreased IL4-induced expression when *Trem2* expression was decreased. LPS-induced pro-inflammatory stimulation suppressed *Trem2* expression, thus preventing TREM2's anti-inflammatory drive. The importance of *Trem2* activity in regulating the pro- and anti-inflammatory balance of microglia, particularly mediating effects of the IL4-regulated anti-inflammatory pathway, has important implications for fighting neurodegenerative disease.

Key words:

TREM2, microglia, Alzheimer's, inflammation, interleukin, STAT6, Arginase

bioRxiv preprint first posted online Oct. 22, 2018; doi: http://dx.doi.org/10.1101/449884. The copyright holder for this preprint (which was not peer-reviewed) is the author/funder, who has granted bioRxiv a license to display the preprint in perpetuity. All rights reserved. No reuse allowed without permission.

Table of contents image

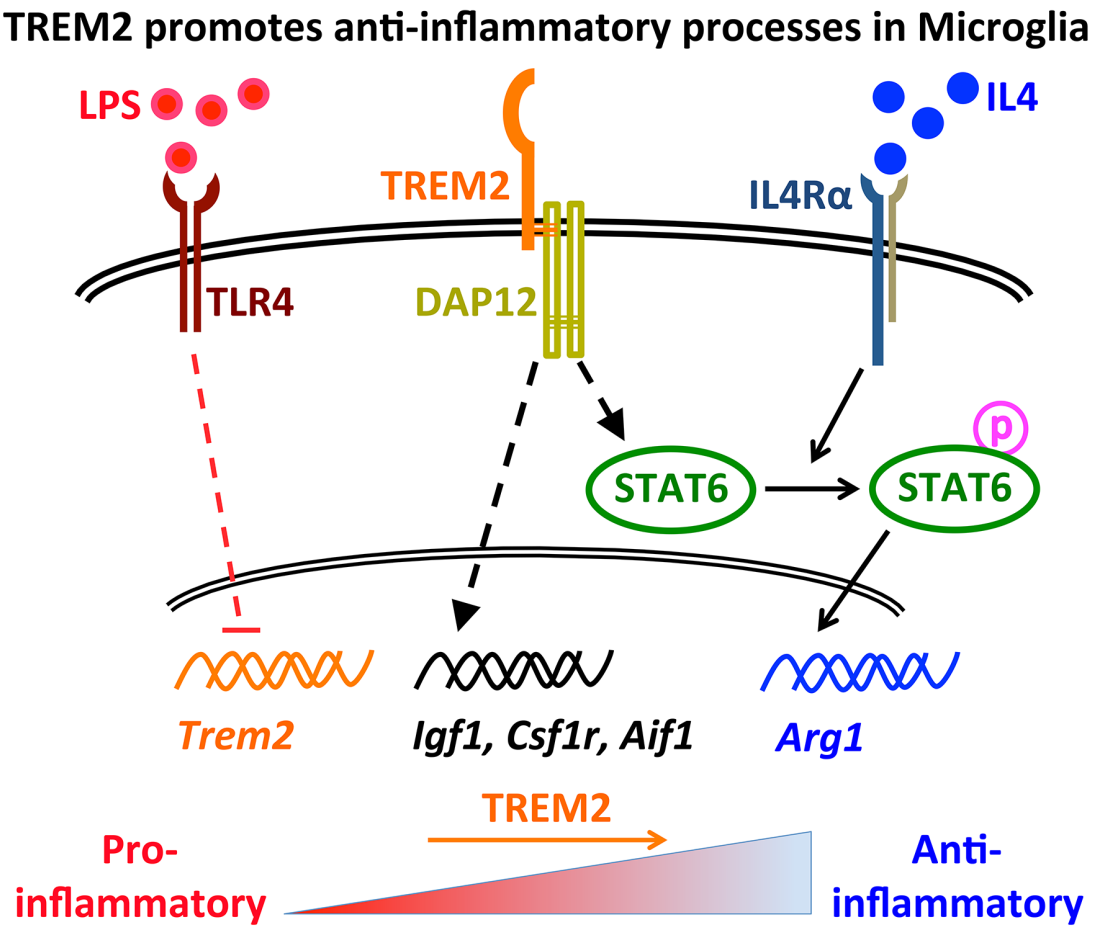

Main points

TREM2 coordinates anti-inflammatory processes in primary microglia, in part by promoting IL4-STAT6 signaling. LPS-induced pro-inflammatory stimulation suppresses *Trem2*. *Trem2* R47H knock-in mice showed a decrease of microglial density in hippocampus.

bioRxiv preprint first posted online Oct. 22, 2018; doi: http://dx.doi.org/10.1101/449884. The copyright holder for this preprint (which was not peer-reviewed) is the author/funder, who has granted bioRxiv a license to display the preprint in perpetuity. All rights reserved. No reuse allowed without permission.

1. Introduction

Genome-wide association studies (GWAS) continue to reveal variants in immune/microglia-related genes that significantly increase the risk of developing Alzheimer's disease (AD). These genes now include *TREM2*, *CD33*, *ABI3* and *PLCG2* (Griciuc et al. 2013; Guerreiro et al. 2013b; Hollingworth et al. 2011; Jonsson et al. 2013; Malik et al. 2013; Naj et al. 2011; Sims et al. 2017). These studies particularly emphasize an important role of microglia in AD pathogenesis. However, the question of how microglial activation contributes to AD development is still far from resolved. Nor is it clear how to use these findings to leverage microglial pathways for drug discovery.

Triggering receptor expressed on myeloid cells 2 (TREM2) is a transmembrane protein containing a single immunoglobulin-superfamily (Ig-SF) domain. TREM2 expression was first observed in macrophages and dendritic cells, but not granulocytes or monocytes (Bouchon et al. 2000; Bouchon et al. 2001; Daws et al. 2001). It has since been reported to be widely expressed in various cell types derived from the myeloid lineage, such as bone osteoclasts (Humphrey et al. 2006; Paloneva et al. 2003), and lung and peritoneal macrophages (Turnbull et al. 2006). In the brain, *TREM2* is predominantly expressed by microglia (Paloneva et al. 2002; Schmid et al. 2002; Takahashi et al. 2005; Wang et al. 2016). In 2013, two independent GWAS studies (Guerreiro et al. 2013b; Jonsson et al. 2013) highlighted a rare variant rs75932628-T in exon 2 of the *TREM2* gene, causing an arginine-to-histidine substitution at amino acid position 47 (R47H), to be highly significantly associated with increased AD risk. The risk from this variant has a comparable effect size to the *APOEε4* allele (around 3-fold increased AD risk; Benitez et al. 2013; Jin et al. 2014; Jonsson et al. 2013; Murray et al. 2018; Ruiz et al. 2014). Furthermore, the R47H variant was investigated in other neurodegenerative diseases and was also found to be associated with frontotemporal dementia, Parkinson's disease, and amyotrophic lateral sclerosis (Cady et al. 2014; Rayaprolu et al. 2013), suggesting a more

bioRxiv preprint first posted online Oct. 22, 2018; doi: http://dx.doi.org/10.1101/449884. The copyright holder for this preprint (which was not peer-reviewed) is the author/funder, who has granted bioRxiv a license to display the preprint in perpetuity. All rights reserved. No reuse allowed without permission.

widespread role for TREM2-related microglial functions in maintaining neuronal function/survival throughout the brain. In addition to the R47H variant, further *TREM2* variants have been revealed to be risk factors of AD or other CNS diseases, such as R62H (Jin et al. 2014; Sims et al. 2017), H157Y (Jiang et al. 2016), Q33X, T66M and Y38C (Guerreiro et al. 2013a; Guerreiro et al. 2013c). All of the *TREM2* genetic linkage studies with neurodegenerative diseases suggest an important contribution of TREM2 to regulating microglial functions with respect to neuronal function/survival in the process of disease progression.

Evidence from *in vitro* studies has accumulated to support the role of TREM2 in restricting inflammation and promoting phagocytosis. It was first reported in a study using primary microglia transduced with flag epitope tagged TREM2 that TREM2 stimulated microglial chemotaxis, and phagocytosis of fluorescent beads (Takahashi et al. 2005). They also showed that *Trem2* knockdown via a lentiviral strategy increased pro-inflammatory gene expression and decreased phagocytosis of labeled apoptotic neuronal membranes in primary microglia stressed with co-culture of apoptosis-induced primary neurons. TREM2 was also found to inhibit LPS-induced pro-inflammatory markers up-regulated in primary alveolar macrophages *in vitro* (Gao et al. 2013), and the BV-2 microglial cell line (Zhong et al. 2015). With particular respect to AD, phagocytosis of Aβ was found to be impaired due to lack of or reduced mature TREM2 cell surface expression in studies with primary microglia from *Trem2* knock-out mice and mutant *Trem2* microglial cell lines (Kleinberger et al. 2014; Xiang et al. 2016). Recently, it was further shown that apolipoproteins and Aβ itself acted as ligands of TREM2 to facilitate microglial phagocytosis and clearance of Aβ and apoptotic neurons (Atagi et al. 2015; Yeh et al. 2016; Zhao et al. 2018). In general, these studies suggest that *Trem2* deficiency exacerbates microglial pro-inflammatory activation in response to various stimuli, and accompanies impaired phagocytosis. However, other cellular functions of TREM2, particularly anti-inflammatory or alternative activation, and the molecular mechanisms mediating the actions of TREM2 are not well understood.

bioRxiv preprint first posted online Oct. 22, 2018; doi: http://dx.doi.org/10.1101/449884. The copyright holder for this preprint (which was not peer-reviewed) is the author/funder, who has granted bioRxiv a license to display the preprint in perpetuity. All rights reserved. No reuse allowed without permission.

In this study, we developed a strategy to investigate the role of microglial-expressed genes that alter risk for AD in microglia using primary cultures and acute knockdown of gene expression using RNAi, and also verifying our findings in mouse brain. We used this strategy to explore the effects of acute *Trem2* deficiency on primary microglia at the transcriptional and functional levels, especially when polarized towards a pro-inflammatory or anti-inflammatory phenotype. We aimed to compare the effect of acute siRNA-induced knockdown of *Trem2* expression to loss-of-function due to the R47H mutation by comparing both cultures of isolated microglia and brain tissue from wild-type (WT) or recently developed mice carrying the *Trem2* R47H point mutation from the Jackson laboratories (*Trem2* R47H knock-in mice, KI mice). The primary effect reported in the R47H mice was a similar reduction of *Trem2* expression, and this effect was also observed in independent *Trem2 R47H* KI mice (Cheng-Hathaway et al. 2018; Xiang et al. 2018). The changes in *Trem2*-mediated effects in this mouse seem to be largely due to this decrease of *Trem2* expression rather than due to the mutation and so this effectively provides us with an *in vivo* 'knockdown' model without the need for further intervention, providing a control without transfection, and the possibility of verifying effects *ex vivo*. We find both *in vitro* and *in vivo* that decreased levels of *Trem2* have effects on microglial function and gene expression. We investigate the pro- versus anti-inflammatory effects of *Trem2* and investigate possible molecular pathways mediating these effects.

bioRxiv preprint first posted online Oct. 22, 2018; doi: http://dx.doi.org/10.1101/449884. The copyright holder for this preprint (which was not peer-reviewed) is the author/funder, who has granted bioRxiv a license to display the preprint in perpetuity. All rights reserved. No reuse allowed without permission.

2. Materials and Methods

2.1. Mice

All experiments were performed in agreement with the Animals (Scientific Procedures) Act 1986, with local ethical approval. *Trem2* R47H knock-in (R47H KI) mice were obtained from the Jackson Laboratory (C57BL/6J-*Trem2*^{em1Adiuj}/J; stock number: 027918, RRID: IMSR_JAX:027918; Xiang et al. 2018), and maintained on a C57BL/6J background. All mice were bred and maintained at UCL on a 12 hr light/12 hr dark cycle with *ad libitum* supply of food and water. Genomic DNA was extracted for genotyping using the 'HotSHOT' lysis method. Alkaline lysis reagent (25 mM NaOH, 0.2 mM EDTA [pH 12]) was added to tissue samples prior to heating to 95°C for 30 min. The sample was then cooled to 4°C before the addition of neutralization buffer (40 mM Tris-HCl [pH 5]). Mice were genotyped using a quantitative PCR reaction utilizing the following primers and probes (Thermo Fisher Scientific):

Forward primer 5' ACT TAT GAC GCC TTG AAG CA 3',
Reverse primer 5' CTT CTT CAG GAA GGC CAG CA 3',
wild-type probe 5' VIC- AGA CGC AAG GCC TGG TG -MGBNFQ 3',
mutant probe 5' 6-FAM- AGA CAC AAA GCA TGG TGT CG -MGBNFQ 3'

TaqMan genotyping master mix was used according to the manufacturer's instructions.

2.2. Primary microglial culture

Primary microglial cultures were generated from cerebral cortices and hippocampi of 1-3-day-old newborns from WT C57BL/6J or *Trem2* R47H KI mouse strains, following an adapted protocol of Schildge et al. (2013) and Saura et al. (2003). For each independent preparation of WT primary microglial culture, brains of 4-6 pups from one litter of neonatal mice were dissected and pooled. For the *Trem2* KI mice, primary cultures from 2-4 pups from the same litter were prepared simultaneously but cultured separately,

bioRxiv preprint first posted online Oct. 22, 2018; doi: http://dx.doi.org/10.1101/449884. The copyright holder for this preprint (which was not peer-reviewed) is the author/funder, who has granted bioRxiv a license to display the preprint in perpetuity. All rights reserved. No reuse allowed without permission.

and genotyping was performed after culture preparation. On average, around 3,000,000~4,000,000 mixed glial cells from the combined cortex and hippocampus per pup were obtained. Specifically, after decapitation, the brain was quickly extracted and transferred to ice-cold HBSS. The cortices and hippocampi from each brain were then isolated by removing all other brain regions, meninges and blood vessels. Following mechanical and enzymatic (HBSS with 0.25% trypsin) dissociation, cells were centrifuged, collected and seeded at a density of 120,000 cells/cm^2 in poly-D-lysine coated flasks/wells with a glial culture medium (high glucose DMEM with 10% heat-inactivated fetal bovine serum, 100 U/ml penicillin and 100 µg/ml streptomycin). Cells were cultured at 37°C in humidified 5% CO_2 and the medium was changed every 3 days. After 19-23 days, once the mixed glial cells achieved confluence, a mild trypsinization method (incubation with DMEM with 0.05% trypsin and 0.2 mM EDTA for 30-45 min) was applied to purify the primary microglia by removing the astrocytic cell layer. Conditioned medium from the mixed glia was collected before trypsinization. Isolated primary microglial cells were collected and seeded in poly-D-lysine coated plates at a density of 40,000-100,000 cells/cm^2 using the collected conditioned medium, except for the cultures used for ELISA, which were cultured in fresh medium. Pure primary microglia were cultured under the same conditions as the mixed glial culture, and experiments were started at 24 hr after isolation.

2.3. Adult mouse brain tissue extraction

Brains were removed from the skull on ice following decapitation, and cut into two hemispheres. The hippocampus and cortex were dissected from one hemisphere and then snap frozen on dry ice and stored at -80°C until total RNA was isolated by homogenisation of tissue with a polytron. The second hemisphere was fixed in 4% paraformaldehyde overnight at 4°C and then cryoprotected and stored in 30% sucrose in phosphate buffered saline (PBS) with 0.02% sodium azide.

bioRxiv preprint first posted online Oct. 22, 2018; doi: http://dx.doi.org/10.1101/449884. The copyright holder for this preprint (which was not peer-reviewed) is the author/funder, who has granted bioRxiv a license to display the preprint in perpetuity. All rights reserved. No reuse allowed without permission.

2.4. Hippocampal histology

The fixed hemisphere was serially sectioned at 30 µm transverse to the long axis of the hippocampus using a frozen microtome (Leica, Germany). For assessing microglial density and activity, free floating sections were permeabilized in 0.3% Triton-X in PBS three times, blocked (3% goat serum in 0.3% Triton X-100 in PBS) for 1 hr at room temperature and incubated with primary antibodies at 1:500 dilution in blocking solution (IBA1 rabbit antibody, #234003, Synaptic Systems, RRID: AB_10641962; CD68 rat antibody, #MCA1957, Bio Rad, RRID: AB_322219), overnight at 4°C. Sections were washed, then incubated for 2 hr at room temperature with corresponding Alexa-conjugated secondary antibodies diluted to 1:800 in blocking solution (goat anti-rabbit Alexa 488 and goat anti-rat Alexa 594 antibodies, Jackson ImmunoResearch). Sections were washed, nuclei counterstained with 4',6-diamidine-2-phenylindole (DAPI), then mounted with Fluoromount-G medium (Southern Biotech). Entire hippocampus was imaged in each section using an EVOS FL Auto microscope (Life Technologies) with a x20 objective, by area defined serial scanning and a motorised stage. For AIF1 and CD68 staining, cells were counted in the CA1: *stratum radiatum* in subfields of size 91,100 μm^2, *stratum lacunosum-moleculare* (subfield 68,300 μm^2), *stratum pyramidale* and *stratum oriens* (subfields 76,900 μm^2). Microglial cells were only counted if their DAPI-stained nucleus could be clearly seen surrounded by AIF1 staining with at least two processes protruding from this, and more than 50% of the cell body being present in the subfield. CD68 positive cells were characterized by the cell body containing greater than 25% fluorescence. At least three serial hippocampal sections approximately 720 µm apart were counted for each mouse. Experimenter was blind to the age and genotype of the sample during quantification and analysis.

2.5. BV-2 cell culture

BV-2 cells (maximum passage number < 20), a murine microglial cell line, were cultured in medium containing DMEM with 10% heat-inactivated fetal

bioRxiv preprint first posted online Oct. 22, 2018; doi: http://dx.doi.org/10.1101/449884. The copyright holder for this preprint (which was not peer-reviewed) is the author/funder, who has granted bioRxiv a license to display the preprint in perpetuity. All rights reserved. No reuse allowed without permission.

bovine serum, 2 mM L-glutamine, 100 U/ml penicillin, 100 µg/ml streptomycin, and 1% mycoplasma removal agent (AbD Serotec), and passaged every 2-4 days (avoiding confluence of more than 90%). Prior to experiments, BV-2 cells were collected with Accutase (A6964, Sigma), and seeded on 6-well plates at a density of around 10,000 cells/cm^2 for testing siRNA sequences.

2.6. siRNA treatment

The following three siRNAs (Ambion) that target mouse *Trem2* were tested (with a non-targeting siRNA as a control, Ambion, Catalog No. 4457287):

siRNA No. 1 sequences: sense 5'-CCCUCUAGAUGACCAAGAUtt-3', antisense 5'-AUCUUGGUCAUCUAGAGGGtc-3';
siRNA No. 2 sequences: sense 5'-GCGUUCUCCUGAGCAAGUUtt-3', antisense 5'-AACUUGCUCAGGAGAACGCag-3';
siRNA No. 3 sequences: sense 5'-GCACCUCCAGGAAUCAAGAtt-3', antisense 5'-UCUUGAUUCCUGGAGGUGCtg-3')

Nuclease-free water was used to make 20 µM siRNA solutions. The 3 *Trem2* siRNAs were tested in BV2 cells and the siRNA No. 2 and No. 3 were selected for *Trem2* knockdown in primary microglia.

Primary mouse microglia were transfected with either *Trem2* siRNA or the non-targeting negative control siRNA using the transfection reagent Lipofectamine RNAiMax (Invitrogen), following the manufacturer's instructions. The amount of siRNA to volume of Lipofectamine per well was 1 pmol siRNA to 0.3 µl Lipofectamine. Cells were harvested 72±2 hr after transfection.

bioRxiv preprint first posted online Oct. 22, 2018; doi: http://dx.doi.org/10.1101/449884. The copyright holder for this preprint (which was not peer-reviewed) is the author/funder, who has granted bioRxiv a license to display the preprint in perpetuity. All rights reserved. No reuse allowed without permission.

2.7. LPS or IL4 treatment

For the microglial activation studies, primary microglia were treated with 1 µg/ml lipopolysaccharides (LPS; L4391, Sigma) at 3, 6, or 24 hr before harvest, or 20 ng/ml Interleukin 4 (IL4; 214-14, PeproTech) at 24 or 48 hr before harvest. Time points for the addition of LPS or IL4 treatment are given in Figure 1.

2.8. Phagocytosis assay

The phagocytosis assay using the pHrodo green *E. coli* bioparticles conjugate (P35366, Invitrogen) was adapted from the Invitrogen protocol (Garcia-Reitboeck et al. 2018; Kleinberger et al. 2014). In brief, purified primary microglia were cultured on 24-well plates at a density of around 50,000 cells/cm^2 (100,000 cells/well) and transfected with either *Trem2* siRNA or the negative control siRNA. After 72 hr, microglia were treated with 50 µg pHrodo-conjugated *E. coli* per well for 1 hr at 37°C. Cells pre-incubated with 10 µmol cytochalasin-D for 30 min prior to the phagocytosis assay were used as a negative control. Cells were re-suspended with PBS after the assay, and then washed and collected in ice-cold fluorescence-activated cell sorting (FACS) buffer (PBS without $Ca^{2+/}Mg^{2+}$, with 0.5% BSA, 0.05% sodium azide and 2 mM EDTA). Collected microglia were assessed (10,000 cells counted per sample) by flow cytometry (FACSCalibur running CellQuest Pro; Becton Dickinson, UK) with excitation at 488 nm and emission at a range of 500-535 nm. Following identification of single microglial cells with the expected size and granularity by forward (FSC-H) versus side (SSC-H) scatter of light, microglia with different amounts of phagocytosed fluorescent *E. coli* and thus with different fluorescent intensities were plotted and analyzed using Flowing software (developed by Perttu Terho, Turku Centre for Biotechnology, Finland; www.flowingsoftware.com).

bioRxiv preprint first posted online Oct. 22, 2018; doi: http://dx.doi.org/10.1101/449884. The copyright holder for this preprint (which was not peer-reviewed) is the author/funder, who has granted bioRxiv a license to display the preprint in perpetuity. All rights reserved. No reuse allowed without permission.

2.9. Primary microglia lysis for gene expression and protein analysis

For gene expression analysis, primary microglia were washed with ice-cold PBS three times and then lysed in ice-cold QIAzol RNA lysis reagent (Qiagen). Lysed cells were snap frozen on dry ice and stored at -80°C.

To analyze cellular protein, primary microglia were washed with ice-cold PBS three times and then lysed in 2X Laemmli dye. Lysed cells were boiled at 95°C in a heating block for 5 min and stored at -20°C.

For ELISA analyses, supernatants from primary microglial culture were collected, centrifuged to remove cell debris and stored at -20°C.

2.10. RNA purification and cDNA preparation

Prior to RNA purification, the primary microglia samples were homogenized using a 1 ml syringe and a G21 needle, or hippocampal samples were homogenized using a polytron. Total RNA was isolated using miRNAeasy columns (Qiagen) following manufacturer's instructions. The concentration of RNA was assessed with a NanoDrop Spectrophotometer (Thermo Scientific), with the A_{260}/A_{280} ratio typically around 2. Randomly selected RNA samples from different experiments (*Trem2* knockdown and non-targeting siRNA, or from *Trem2* R47H mice and WT siblings; n = 6 per group), were tested by capillary electrophoresis to confirm the quality and concentration of the total RNA (Supplementary Figure 1). Typical RNA Integrity values (RIN) of >9.0 from 10.0 were obtained regardless of siRNA treatment type, or genotype of mice.

The same amount of RNA from each sample was first treated using DNase I (Amplification Grade, Invitrogen) plus RNaseOUT (Invitrogen). The reverse transcription reaction was then performed using the High Capacity cDNA Reverse Transcription Kit with RNase Inhibitor (Applied Biosystems) following

bioRxiv preprint first posted online Oct. 22, 2018; doi: http://dx.doi.org/10.1101/449884. The copyright holder for this preprint (which was not peer-reviewed) is the author/funder, who has granted bioRxiv a license to display the preprint in perpetuity. All rights reserved. No reuse allowed without permission.

the manufacturer's instructions, in parallel with a negative control lacking the reverse transcriptase.

2.11. Primer design and test

Primers were designed to span at least two exons and tested for specificity against the entire mouse transcriptome using Primer-BLAST (NCBI) and supplied by Eurofins MWG Operon. All primers were tested for specificity by performing a standard PCR reaction and resolving the products on a 3% agarose gel with ethidium bromide, followed by a quantitative RT-PCR reaction to obtain the linearity range for primers, calculate primer efficiency and test primer specificity using a "melt-curve" analysis. All primer sequences are listed in Supplementary Table 1.

2.12. RT-qPCR

The cDNA samples were tested in triplicate with a reverse-transcriptase (RT) lacking control in a 96-well plate using the CFX96 system (BioRad), with each 20 µl reaction containing the cDNA dilution, 0.25 µM of forward and reverse primers, and SYBR Green PCR master mix (Bio-Rad). Cycling conditions were: 95°C-3 min, 40 cycles of [95°C-10 sec, 58°C-30 sec and 72°C-30 sec], and then 72°C-5 min. A melt curve was generated by heating from 60 to 90°C with 0.5°C increments and 5 sec dwell time. All RT-qPCR reactions were checked for a single peak with the melt-curve analysis reflecting a single PCR product. Expression levels of the housekeeping gene *Rps28* were shown to be stable between the different experimental samples when higher molecular weight RNA was measured (Supplementary Figure 1). The raw cycle threshold (CT) values of target genes (mean of the triplicates for each sample) were normalized to *Rps28* CT values for each sample using the delta CT method (Matarin et al. 2015).

bioRxiv preprint first posted online Oct. 22, 2018; doi: http://dx.doi.org/10.1101/449884. The copyright holder for this preprint (which was not peer-reviewed) is the author/funder, who has granted bioRxiv a license to display the preprint in perpetuity. All rights reserved. No reuse allowed without permission.

2.13. ELISA of secreted TNF-alpha by primary microglia

The TNF-alpha levels in the primary microglial supernatants were quantified using Quantikine® Mouse TNF-alpha ELISA kit (R&D Systems, MTA000B), following the manufacturer's instructions. In general, equal volumes of cell supernatants, together with the provided buffer, were loaded in duplicate to the ELISA microplate and incubated for 2 hr at room temperature. Following five washes, wells were then incubated with horseradish peroxidase conjugated mouse TNF-alpha antibody for another 2 hr at room temperature. The microplate was washed again and incubated with a substrate solution prepared with chromogen (tetramethylbenzidine) and hydrogen peroxide for 30 min before addition of a stop solution with hydrochloric acid. Then the color intensity was measured at 450 nm using a plate reader (EL800, BioTek) and the TNF-alpha concentrations in microglial supernatants were calculated from the standard curve. To account for the differences in the cell number between different wells of microglia, cell lysates were collected in parallel with the supernatants from the same wells and then tested for levels of a housekeeping protein beta-actin (Ab8227, Abcam, RRID: AB_2305186) by western blot, which was used for normalization of TNF-alpha levels.

2.14. Western blotting

Cellular protein samples from primary microglia were loaded onto 15% polyacrylamide gels and resolved by sodium dodecyl sulfate polyacrylamide gel electrophoresis. Proteins were transferred to a 0.45 μm nitrocellulose membrane (BioRad) by wet electro-transfer overnight.

Membranes were washed in Tris-buffered saline (TBS; 30 mM NaCl and 30 mM Tris [pH 7.4]) for 10 min, and then blocked in TBS with 0.1% Tween-20 (TBST) and 5% non-fat milk for 1 hr at room temperature. Membranes were then probed with primary antibody (STAT6 antibody, 5397S, Cell Signaling Technology, RRID: AB_11220421; p-STAT6 (Y641) antibody, 56554S, Cell Signaling Technology; AKT (pan) antibody, 4691T, Cell Signaling Technology,

bioRxiv preprint first posted online Oct. 22, 2018; doi: http://dx.doi.org/10.1101/449884. The copyright holder for this preprint (which was not peer-reviewed) is the author/funder, who has granted bioRxiv a license to display the preprint in perpetuity. All rights reserved. No reuse allowed without permission.

RRID: AB_915783; p-AKT (T308) antibody, 2965S, Cell Signaling Technology, RRID: AB_2255933; p-AKT (S473) antibody, 4060T, Cell Signaling Technology, RRID: AB_2315049; beta-actin antibody, ab8227, Abcam, RRID: AB_2305186) diluted in blocking buffer overnight at 4°C. Following three washes with TBST, membranes were then incubated with a horseradish peroxidase conjugated secondary antibody that was diluted 1:10,000 in blocking buffer for 1 hr at room temperature. Membranes were finally washed 3 more times, and the horseradish peroxidase signals revealed with enhanced chemiluminescence detection (ECL, BioRad). Image acquisition and densitometric analysis was performed using ImageLab (v5.2, BioRad).

2.15. Immunocytochemistry

Primary microglia plated on poly-D-lysine coated coverslips were fixed with 2% PFA for 15 min at room temperature, followed by five washes with PBS. Prior to immunocytochemical staining, coverslips were washed in PBS for 10 min and blocked for 1 hr at room temperature with 8% horse serum diluted in PBS with 0.125% Triton-X 100. Coverslips were then incubated overnight at 4°C with IBA1 antibody (019-19741, Wako, RRID: AB_839504) diluted 1:1,000 in the blocking solution. After primary antibody incubation, coverslips were washed three times with PBS and then incubated for 2 hr at room temperature in the anti-rabbit secondary antibody dilution in blocking solution. After three washes with PBS and staining with DAPI, coverslips were mounted on SuperFrost Plus slides (Fisher) with Fluoromount G (Scientific Biotech).

2.16. Imaging and analysis

Coverslips were imaged using an EVOS® FL Auto Cell Imaging System (Life Technologies) under a 20X objective. Two coverslips per sample were used and three fields of view (480 µm x 360 µm) per coverslip were imaged. AIF1-positive cells and DAPI were counted with Adobe PhotoShop CS6 software

bioRxiv preprint first posted online Oct. 22, 2018; doi: http://dx.doi.org/10.1101/449884. The copyright holder for this preprint (which was not peer-reviewed) is the author/funder, who has granted bioRxiv a license to display the preprint in perpetuity. All rights reserved. No reuse allowed without permission.

and the microglial purity was calculated as a percentage of the AIF1 cell counts versus the DAPI counts in the same field of view.

2.17. Statistics

Data are shown as mean ± SEM. The sample size (n) represents the number of independent cell preparations or mice. All statistics were performed using Prism v7 (Graphpad). For the primary microglial gene expression changes with *Trem2* knockdown versus the non-targeting siRNA control, single gene expression level was normalized as a fold change of the negative control within each independent microglial culture preparation, and then a one-sample Student's *t*-test with Bonferroni correction was conducted for statistical analysis. For the phagocytosis experiment, a paired Student's *t*-test was used to compare the *Trem2* knockdown group and the non-targeting siRNA control group (samples from the same microglial culture preparation were paired). For the LPS or IL4 treatment experiments, to assess the impact of *Trem2* knockdown and LPS/IL4 treatment on the gene expression, data were normalized to the negative control without LPS/IL4 treatment within each individual microglial preparation and then analyzed with two-way ANOVA followed by Sidak's multiple comparison tests when appropriate. The *Trem2* R47H KI expression data in whole hippocampal homogenates were tested by one-way ANOVA with Sidak's multiple comparisons tests when appropriate. The *Trem2* R47H KI immunohistochemistry data were analyzed using two-way ANOVA with Sidak's multiple comparisons tests when appropriate. For the primary microglia cultured from the *Trem2* R47H KI mice, data were analyzed with two-way ANOVA separately for LPS or IL4 treatment using the same control samples, then Sidak's multiple comparisons tests were performed when appropriate. Differences were considered significant if $p<0.05$.

bioRxiv preprint first posted online Oct. 22, 2018; doi: http://dx.doi.org/10.1101/449884. The copyright holder for this preprint (which was not peer-reviewed) is the author/funder, who has granted bioRxiv a license to display the preprint in perpetuity. All rights reserved. No reuse allowed without permission.

3. Results

3.1. Establishing an *in vitro* model of acute *Trem2* knockdown

To investigate the functional importance of microglial genes, reported to have variants altering risk for AD from GWAS experiments, we established an *in vitro* model where primary microglia were kept in mixed glial culture conditions to fully develop for around 21 days before isolation. We used this model to elucidate the implications of acute *Trem2* knockdown (Figure 1a). The purity of our primary microglial culture was validated via immunocytochemistry against IBA1 alongside total cell counts from DAPI nuclei staining (97.2±0.3% IBA1-positive cells; Figure 1b). Additionally, consistent with previous descriptions (Saura et al. 2003), the majority of the microglia showed a typical elongated morphology (bipolar or unipolar), with a small proportion of ameboid cells. In order to validate the capacity of the microglial culture to be polarized in the direction of either the pro- or anti- inflammatory phenotype, LPS or IL4 was applied respectively, and expression of typical pro-inflammatory (*Tnf* and *Il1b*) or anti-inflammatory (*Arg1* and *Tgfb1*) genes were analyzed via RT-qPCR (Figure 1c). Microglia without LPS expressed low transcriptional levels of *Tnf* and *Il1b*; while with LPS treatment we observed a remarkable increase in the mRNA levels of *Tnf* and *Il1b*, presenting as early as 3 hr after LPS application, and around 100-fold up-regulation of *Tnf* and 1,500-fold of *Il1b* at 24 hr. In contrast, IL4 treatment induced a significant time-dependent up-regulation of *Arg1* and *Tgfb1* expression (Figure 1c). *Arg1* expression, undetectable in our non-stimulated microglia, reached levels well above detection threshold at 24 hr after IL4 treatment, and by 48 hr expression levels had further doubled. *Tgfb1* expression showed up-regulation to around 120% of non-stimulated levels at 24 hr and 130% at 48 hr. These expected changes in *Tnf* and *Il1b*, and *Arg1* and *Tgfb1*, serve to validate that LPS and IL4 can be used in this system of primary microglia to promote a pro-inflammatory and anti-inflammatory fate, respectively.

bioRxiv preprint first posted online Oct. 22, 2018; doi: http://dx.doi.org/10.1101/449884. The copyright holder for this preprint (which was not peer-reviewed) is the author/funder, who has granted bioRxiv a license to display the preprint in perpetuity. All rights reserved. No reuse allowed without permission.

3.2 Acute *Trem2* knockdown in primary microglia is effective and impairs phagocytosis, validating the preparation

To determine the efficiency of *Trem2* knockdown, BV-2 cells were transfected with different *Trem2* siRNA sequences plus Lipofectamine. Transfected cells were collected at 24 and 48 hr and assessed for *Trem2* expression levels by RT-qPCR (Figure 2a). Three different siRNA sequences against *Trem2* were tested in parallel to a non-targeting control siRNA. The most effective siRNA (sequence 2) gave >80% knockdown of *Trem2* mRNA levels compared to the non-targeting siRNA control. Thus we chose this sequence for the RNAi experiments in primary microglia. The next most effective siRNA against *Trem2* was sequence 3, giving 50-60% knockdown of *Trem2*; this second siRNA was used to confirm that key findings in the primary microglia were dependent on the levels of *Trem2* expression (Supplementary Figure 2).

The *Trem2* knockdown in the primary microglia performed consistently well (Figure 2b), and an average decrease of 79.2±1.1% in the *Trem2* mRNA levels was obtained. It is, however, interesting to note that basal *Trem2* levels in the primary microglia were very varied but in all cases *Trem2* knockdown was effective.

To assess the effect of *Trem2* knockdown in this system, we initially tested the effects on phagocytosis. Previous studies have already shown impaired phagocytosis in primary microglia isolated from *Trem2* knockout mice and cell lines transfected with FTD-like or AD-associated *TREM2* mutations (Kleinberger et al. 2014) as well as with *Trem2* knockdown in primary microglial culture (Takahashi et al. 2005) or in human microglia-like cells from induced pluripotent stem cells harboring *TREM2* mutations associated with Nasu-Hakola dementia (Garcia-Reitboeck et al. 2018). Here we investigated if acutely induced *Trem2* deficiency via RNAi in the preparation of primary microglia used in the present study showed a similar impairment. A phagocytosis assay was performed 72 hr after siRNA transfection, to test the ability of microglia to phagocytose pHrodo (a pH-sensitive fluorescent dye), conjugated to *E. coli,* followed by quantification of the microglia containing the

bioRxiv preprint first posted online Oct. 22, 2018; doi: http://dx.doi.org/10.1101/449884. The copyright holder for this preprint (which was not peer-reviewed) is the author/funder, who has granted bioRxiv a license to display the preprint in perpetuity. All rights reserved. No reuse allowed without permission.

fluorescent bacteria in lysosomes by FACS. As a negative control, phagocytosis was inhibited with cytochalasin D (a potent inhibitor of actin polymerization) before addition of *E. coli*. We found that microglia with *Trem2* knockdown showed a significant reduction (48.1±9.1%) of phagocytosis compared to the non-targeting siRNA treated microglia, confirming previous reports and further validating this cell system (Figure 2c).

3.3. Acute *Trem2* knockdown causes transcriptional changes in primary microglia.

To understand the genetic pathways regulated by TREM2, we next investigated the subsequent gene expression changes in microglia caused by *Trem2*-knockdown. We initially tested canonical microglial marker genes alongside those we previously found to be potentially implicated in AD in the same genetic network as *Trem2,* following a microarray study of AD-associated mouse models (Matarin et al. 2015), or genes that have been implicated in AD. We initially observed that *Trem2* knockdown was accompanied by decreased expression of the microglial marker *Aif1* compared to the control-treated group within each culture preparation (Figure 3). Note that, as these are almost pure microglia cultures, as outlined above, the decrease in *Aif1* expression relative to the housekeeping gene represents a decrease on average per microglial cell rather than a decrease in the number of microglia, although this may also occur. This decreased level of *Aif1* expression relative to the housekeeping gene in *Trem2* knockdown microglia is consistent with previous evidence that *Aif1* is involved in phagocytosis (Ohsawa et al. 2000). We then found that *Trem2* knockdown resulted in a significant down-regulation of a number of microglial genes at 72 hr after siRNA transfection including *C1qa, Cd68, Csf1r, Igf1, Pik3cg, Spi1, Tnf and Tgfb1* (Figure 3), suggesting that *Trem2* is required to maintain the levels of these genes under non-stimulated conditions *in vitro*. It is interesting to note that *Csf1* receptor is known as a survival and developmental factor for microglia (Elmore et al. 2014; Ginhoux et al. 2010), and so this could be associated with a decreased survival of microglia after *Trem2* knockdown. Interestingly, we saw that the levels of some microglial-specific genes such as

bioRxiv preprint first posted online Oct. 22, 2018; doi: http://dx.doi.org/10.1101/449884. The copyright holder for this preprint (which was not peer-reviewed) is the author/funder, who has granted bioRxiv a license to display the preprint in perpetuity. All rights reserved. No reuse allowed without permission.

Plcg2 and *Il1b* were not significantly altered when *Trem2* expression was knocked down, indicating that *Trem2* is not required to maintain the expression of all microglial gene expression. Overall, acute *Trem2* knockdown produced a significant change in the gene expression profile of microglia under non-stimulated conditions, which might result in a shift of the microglial functional phenotype.

3.4. LPS stimulation dramatically suppresses *Trem2* gene expression in primary microglia.

An important outstanding question is how *Trem2* is regulated; our previous work in transgenic mouse models associated with AD showed that the expression levels of *Trem2* were increased up to 6-fold in tight correlation with amyloid pathology (Matarin et al. 2015). To begin to investigate how *Trem2* expression is regulated, microglia were stimulated with LPS to induce classical pro-inflammatory responses. We first found that, in the control cells, LPS treatment strongly down-regulated *Trem2* expression (Figure 4a), which was consistent with the previous findings in primary mixed glial cell cultures and peritoneal macrophage cell cultures (Schmid et al. 2002) and primary microglia (Owens et al. 2017). The time course analysis showed that the *Trem2* expression started to drop to around 90% of the levels measured in non-stimulated cells from as early as 3 hr after LPS addition, and then continued decreasing and reached levels as low as 10% of non-stimulated levels by 24 hr. This suggests that pro-inflammatory conditions inhibit microglial *Trem2* expression, which might result in a state of temporary or chronic 'TREM2-deficiency' in microglia.

The expression levels of *Tnf* and *Il1b,* two typical pro-inflammatory markers, were greatly increased in our LPS-treated microglia from as early as 3 hr after LPS application. As expected, considering so little *Trem2* remained under these conditions, knockdown of *Trem2* had little effect on LPS-induced gene expression with up-regulation of *Tnf* or *Il1b* being unchanged at the transcriptional level with *Trem2* knockdown compared to control cultures

bioRxiv preprint first posted online Oct. 22, 2018; doi: http://dx.doi.org/10.1101/449884. The copyright holder for this preprint (which was not peer-reviewed) is the author/funder, who has granted bioRxiv a license to display the preprint in perpetuity. All rights reserved. No reuse allowed without permission.

(Figure 4b). It is, however, interesting to note that the up-regulation of *Tnf* and *Il1b* happened considerably more rapidly than the down-regulation of *Trem2*, with *Trem2* knockdown not affecting the dramatic increase in expression of these genes at 3 hr when *Trem2* was only slightly affected by LPS treatment. This may suggest that these pathways are unconnected under these conditions. We further investigated whether the protein level of TNF-alpha released from the microglia 24 hours after LPS treatment was affected by acute *Trem2* knockdown. Consistent with the transcriptional results, ELISA analysis of the microglial-conditioned medium showed that LPS strongly up-regulated microglial TNF-alpha production, but there was no significant change caused by *Trem2* knockdown (Figure 4c).

Considering the time-dependent knockdown of *Trem2* by LPS, we were interested to investigate the effects of this pro-inflammatory treatment on the genes that we had previously tested for effects of *Trem2* knockdown under non-stimulated conditions (Figure 4d). Genes such as *C1qa* and *Igf1* showed a similar pattern of significant time-dependent down-regulation to that of *Trem2* with LPS stimulation. Expression of *Cd68* and *Csf1r*, which were strongly down-regulated by siRNA-induced knockdown of *Trem2* showed a trend towards also being down-regulated in response to the LPS stimulation. In contrast, expression of the *Spi1* (PU.1) transcription factor in the microglia with LPS showed at least a 3.5-fold increase in levels compared to that in the control group, which was observed to start as soon as 3 hr after application, and maintained until at least 24 hr. *Spi1* expression levels were decreased by *Trem2* knockdown, regardless of the LPS-treatment. *Aif1* expression was also increased by LPS stimulation but this only occurred after 24 hours and was again independent of *Trem2* knockdown. *Pik3cg* expression also tended to be up-regulated with LPS, and again *Trem2* knockdown significantly decreased *Pik3cg* expression independent of LPS. Our data with *Spi1, Aif1* and *Pik3cg* suggest that these genes were partially regulated by TREM2, as seen when *Trem2* is knocked down, but can still be induced independently of TREM2 under the condition of LPS treatment, when there is little remaining *Trem2* expression. Together, these data suggest that a major effect of pro-inflammatory LPS stimulation in primary microglia is suppression of *Trem2*

bioRxiv preprint first posted online Oct. 22, 2018; doi: http://dx.doi.org/10.1101/449884. The copyright holder for this preprint (which was not peer-reviewed) is the author/funder, who has granted bioRxiv a license to display the preprint in perpetuity. All rights reserved. No reuse allowed without permission.

expression. In general, the other LPS-dependent effects on gene expression studied here were apparently independent of *Trem2* expression. However, considering the decreased expression of *Trem2* under pro-inflammatory conditions, it is not surprising that siRNA-induced knockdown of *Trem2* had little additional effect. It is possible that *Trem2* regulates expression of these genes and that these effects were thus dependent on the fact that *Trem2* levels were suppressed by LPS.

3.5. *Trem2* is involved in microglial anti-inflammatory responses with IL4

Next we studied the effect of acute *Trem2* knockdown on the alternative anti-inflammatory activation of microglia. IL4 was applied to the cells that had previously been treated either with siRNA against *Trem2* or the non-targeting siRNA, and cells were analyzed at 24 hr and 48 hr after IL4 addition. We first found that microglial *Trem2* expression upon IL4 treatment was maintained at a similar level to that under the basal condition (Figure 5a). As expected, the *Trem2* knockdown group showed significantly lower levels of *Trem2* than the control group. We next investigated two anti-inflammatory markers *Arg1* and *Tgfb1* (Figure 5b). The *Arg1* gene expression was undetectable under non-stimulated conditions by RT-qPCR. Upon IL4 treatment, *Arg1* expression was detectable and showed a time-dependent up-regulation; however, this up-regulation was considerably decreased in the *Trem2*-knockdown group (two-way ANOVA: interaction between main effects of *Trem2* knockdown and IL4 treatment, $p=0.05$). The *Tgfb1* expression also showed an increase with IL4 stimulation, however, in contrast to *Arg1* the effect of *Trem2* knockdown and IL4 showed no interaction.

We went on to compare the effect of the anti-inflammatory stimulus on the gene expression levels of pro-inflammatory markers *Tnf* and *Il1b* (Figure 5c). In contrast to the effect described above for the inflammatory LPS stimulus, the anti-inflammatory IL4 treatment decreased expression of both markers (two-way ANOVA: main effect for IL4 treatment, $p<0.001$ for *Tnf,* and $p<0.01$ for *Il1b*). In the case of *Tnf*, the knockdown of *Trem2* also decreased

bioRxiv preprint first posted online Oct. 22, 2018; doi: http://dx.doi.org/10.1101/449884. The copyright holder for this preprint (which was not peer-reviewed) is the author/funder, who has granted bioRxiv a license to display the preprint in perpetuity. All rights reserved. No reuse allowed without permission.

expression levels but in an IL4-independent manner. In contrast *Trem2* knockdown had no significant effect on *Il1b* expression. Collectively, the IL4-induced microglial response was accompanied by stable *Trem2* expression, and suppressing *Trem2* mRNA levels via RNAi resulted in attenuation of at least part of the anti-inflammatory pathways, which led to a pronounced inhibition of *Arg1* up-regulation. Together these results suggest that *Trem2* tends to push the microglia towards an anti-inflammatory phenotype while a pro-inflammatory stimulus prevents this drive by decreasing *Trem2* expression thus shifting the balance further towards pro-inflammation.

Next, to understand which other genetic pathways are regulated by TREM2 in anti-inflammatory conditions, we investigated the expression of the genes tested previously, but now in response to IL4 (Figure 6). Expression of *C1qa*, *Cd68* and *Igf1* were all found to be significantly up-regulated with IL4 treatment, with tendencies for *Csf1r* and *Spi1* also to increase with IL4, which is similar to what we saw in transgenic mice in correlation with plaque load (Matarin et al. 2015; www.mouseac.org). Neither *Aif1* nor *Plcg2* expression were changed with IL4. Interestingly, the expression of all of these genes was significantly lower in cells with acute *Trem2* knockdown, and was not dependent on IL4 stimulation (no significant interaction of knockdown versus IL4). These data together suggest that the effect of TREM2 on the microglial gene expression profile pushes microglia towards an anti-inflammatory phenotype. However the lack of interaction between the effects of *Trem2* knockdown and IL4 on expression of most of these genes (except *Arg1*) suggests that the effects on these genes are independent parallel pathways which have similar endpoints. Interestingly, the effects of IL4 stimulation on gene expression mimic the changes seen in association with plaque development in transgenic mice where *Trem2* levels are also strongly increased, whereas the pro-inflammatory effects of LPS have the opposite effect.

bioRxiv preprint first posted online Oct. 22, 2018; doi: http://dx.doi.org/10.1101/449884. The copyright holder for this preprint (which was not peer-reviewed) is the author/funder, who has granted bioRxiv a license to display the preprint in perpetuity. All rights reserved. No reuse allowed without permission.

3.6. TREM2 is involved in maintaining normal STAT6 levels in microglia

As microglial *Arg1* up-regulation caused by IL4 stimulation interacted with and was largely suppressed by acute *Trem2* knockdown, we next investigated whether there was an intersection between the IL4 and TREM2 pathways. The phosphorylation of the transcription factor STAT6 is a key step downstream in the IL4 cascade that leads to *Arg1* expression (Gordon and Martinez 2010; Luzina et al. 2012; Nelms et al. 1999). We thus performed western blotting to test whether total or phosphorylated levels of STAT6 were changed in primary microglia with acute *Trem2* knockdown with or without IL4 stimulation (Figure 7a and 7b). We found a slight but significant IL4-induced increase in STAT6 levels but, independent of IL4, knockdown of *Trem2* caused a substantial decrease of the STAT6 total protein levels in the microglia (two-way ANOVA: main effect of IL4-treatment, $p<0.05$; main effect of *Trem2* knockdown, $p<0.0001$, no interaction). IL4 caused robust phosphorylation of STAT6, with phosphorylated STAT6 not detectable in the absence of IL4 but clearly measurable 48 hr after IL4 treatment. *Trem2* knockdown also decreased the total levels of phosphorylated STAT6 but this could be explained by a decrease in the overall levels of STAT6 rather than an effect on phosphorylation *per se*. The expression level of the *Stat6* gene was also decreased with *Trem2* knockdown (Figure 7c), and so confirms the decreased levels of the translated protein. These results suggest that TREM2 deficiency leads to a smaller STAT6 pool in microglia, resulting in decreased amount of phosphorylated STAT6 upon IL4 stimulation. This is consistent with the decrease in IL4-induced *Arg1* expression caused by reduced STAT6-dependent microglial gene transcription in response to decreased *Trem2* expression.

TREM2 signaling is also mediated by the PI3K/AKT pathway (Paradowska-Gorycka and Jurkowska 2013; Zheng et al. 2017), and so we also investigated the effects of *Trem2* knockdown on the AKT signaling in primary microglia (Figure 7d and 7e). Different from the decrease of total STAT6 protein levels, the total AKT protein level was not significantly affected by *Trem2* knockdown, although there was a slight increase in AKT levels in

bioRxiv preprint first posted online Oct. 22, 2018; doi: http://dx.doi.org/10.1101/449884. The copyright holder for this preprint (which was not peer-reviewed) is the author/funder, who has granted bioRxiv a license to display the preprint in perpetuity. All rights reserved. No reuse allowed without permission.

response to IL4 treatment. We then tested activation of AKT, and found that AKT phosphorylation at both Thr308 and Ser473 relative to total AKT was significantly reduced in *Trem2* knockdown microglia (two-way ANOVA: main effect of *Trem2* knockdown, $p<0.01$ for phosphoT308-AKT and $p<0.05$ for phosphoS473-AKT), and this was independent of IL4 stimulation (no interaction between knockdown and IL4). This is not surprising considering that PI3K-AKT signaling is downstream of TREM2, but the unchanged total AKT level suggests that the STAT6 change is not due to general changes in the health and metabolic status of microglia in our cultures.

3.7. Decreased microglial density and down-regulated *Trem2* expression in the hippocampus of *Trem2* R47H knock-in mice

The RNAi strategy allowed us to investigate the general effects of acute *Trem2* 'loss-of-function'. As the risk of AD in humans is greatly increased by variants in the *TREM2* gene, we then aimed to test the effect of the most common of these variants, the R47H mutation, and compare its effects to those of *Trem2* knockdown. We thus employed mice with knock-in of a R47H point mutation into the endogenous mouse *Trem2* gene (Jackson Laboratory, stock # 27918) to study whether the AD-related variant R47H caused similar changes in gene expression, and pro- or anti-inflammatory responses to the RNAi-mediated 'loss-of-function'. The primary effect in these *Trem2* R47H KI mice was a substantial gene dose-related decrease in *Trem2* expression in hippocampal tissue from the mice (Figure 8a). This has subsequently been shown to be due to a splice effect that seems to occur in mice but not in humans (Xiang et al. 2018). Reduced expression of *Trem2* was also seen in an independently generated *Trem2* R47H KI model (Cheng-Hathaway et al. 2018). We can thus consider this R47H mouse line as a good model for verifying the effects of *Trem2* down-regulation *in vivo* to compare to our findings with RNAi-mediated knockdown of *Trem2* presented above. While the down-regulation of the gene together with the mutation is less than ideal for studying the effect of the R47H mutation, comparison of the two models can also give initial information on this subject.

bioRxiv preprint first posted online Oct. 22, 2018; doi: http://dx.doi.org/10.1101/449884. The copyright holder for this preprint (which was not peer-reviewed) is the author/funder, who has granted bioRxiv a license to display the preprint in perpetuity. All rights reserved. No reuse allowed without permission.

In the first instance we investigated the effect of the knockdown in whole tissue from the mouse brain. Considering the decrease in *Csf1r* due to *Trem2* knockdown in the microglial cultures, we hypothesized that microglial numbers and survival may be affected in the *Trem2* R47H mice. To this end, we quantified microglial density in different layers of the hippocampal CA1 region at 4 months of age, using immunohistochemistry with an antibody against IBA1, and found that homozygous *Trem2* R47H KI mice displayed a significant decrease in the number of microglia compared to WT mice, which was consistent in all four CA1 layers (two-way ANOVA: main effect of genotype $p<0.01$; Figure 8b and 8c). Interestingly, we also observed a significant decrease of CD68 positive microglia in the homozygous *Trem2* R47H mice (two-way ANOVA: main effect of genotype $p<0.0001$). This change was not primarily due to the total microglia number change because the proportion of CD68 positive microglia also showed a substantial decrease (two-way ANOVA: main effect of genotype $p<0.001$; Figure 8b and 8c). CD68 (macrosialin) is a lysosomal glycoprotein associated with phagocytosis (Holness and Simmons 1993; Saito et al. 1991). This result suggests that, in addition to slightly reduced microglial density in the hippocampus of homozygous *Trem2* R47H mice, phagocytosis would also be reduced in the surviving microglia. This is consistent with our findings above of reduced phagocytosis in cultured microglia following *Trem2* knockdown.

We assessed the microglial activation status in the hippocampus of R47H *Trem2* KI mice at 4 months of age by investigating the expression of a battery of microglial genes covering pro- and anti-inflammatory functions, and other microglial processes (Figure 8a). Overall, at 4 months of age, a number of genes, shown to be dependent on *Trem2* expression from our knockdown studies above, did not show any significant difference in the hippocampus of the *Trem2* R47H KI mice compared to WT siblings, such as *Aif1, Cd68, Igf1*, *Csf1r* and *Stat6* relative to the *Rps28* housekeeping gene (Figure 8a). It is important to note that in the hippocampal tissue, the gene expression in microglia is greatly diluted by the much greater contribution of other cell types and so small changes in gene expression will be much more difficult to detect

bioRxiv preprint first posted online Oct. 22, 2018; doi: http://dx.doi.org/10.1101/449884. The copyright holder for this preprint (which was not peer-reviewed) is the author/funder, who has granted bioRxiv a license to display the preprint in perpetuity. All rights reserved. No reuse allowed without permission.

than in the primary microglia cultures. However part of the difference is likely also to come from the moderating effects of the mixed cell environment and the activation state of the microglia under these conditions. In summary, the *Trem2* R47H KI mice showed that reduced *Trem2* expression resulted in predominantly a phenotype of a slight but significant decrease in microglial numbers and also lower CD68-positive microglia in the CNS environment of healthy young adult mice. This may prime the mouse for neurodegeneration later in life with aging or other environmental factors.

3.8. Down-regulated *Trem2* expression and impaired *Arg1* induction in primary microglia from *Trem2* R47H knock-in mice

Next, to separate the microglia from other cell types and to compare the effects on gene expression of acute *Trem2* knockdown with siRNA described above to decreased expression throughout the life of the mouse, without the need for transfection, microglia isolated from the *Trem2* R47H mice were stimulated towards a pro- versus anti-inflammatory fate as above. Again, the primary effect in the microglia from the R47H KI mice was a substantial gene dose-related decrease in *Trem2* expression, relative to *Rps28* (Figure 9a), with the microglia isolated from the homozygous *Trem2* R47H mice expressing very similar levels of *Trem2* to the microglia from WT mice after knockdown of *Trem2,* or in the hippocampal tissue from these mice. Also as before, we observed a strong down-regulation of microglial *Trem2* expression in response to LPS treatment, and conversely maintenance of *Trem2* expression with IL4 treatment, which was consistent with our RNAi experiments.

We next investigated whether the decreased expression in microglia from the R47H KI mice caused changes to gene expression in relation to LPS or IL4 treatment. With most genes tested the results obtained were compatible with the effects of the acute siRNA-induced *Trem2* knockdown, described above (Figure 9b, 9c and 10). For LPS treatment the one exception was *Tnf.* In contrast to the acute RNAi experiments in which *Tnf* expression was

bioRxiv preprint first posted online Oct. 22, 2018; doi: http://dx.doi.org/10.1101/449884. The copyright holder for this preprint (which was not peer-reviewed) is the author/funder, who has granted bioRxiv a license to display the preprint in perpetuity. All rights reserved. No reuse allowed without permission.

dramatically increased but with no effect of *Trem2* knockdown, significant changes were seen between the WT and *Trem2* R47H KI mice. After LPS treatment, heterozygous microglia carrying one allele of the *Trem2* R47H showed significantly higher *Tnf* levels compared to WT and homozygous *Trem2* R47H-derived microglia. However as the homozygous R47H cells showed a tendency for reduced *Tnf* expression in non-stimulated conditions, we calculated the fold-change in *Tnf* up-regulation in response to LPS and found that the up-regulation was significantly increased for the homozygous R47H cells (around 200-fold increase) compared to WT (around 150-fold increase). The expression levels for *Il1b* also showed a significant increase in response to LPS, as above, but in this case there was no significant effect of genotype, and so we saw a similar fold-change in *Il1b* up-regulation evoked by LPS for the WT and R47H variant microglia (around 800-fold increase). The difference in the pro-inflammatory gene response to LPS between the *Trem2* knockdown and R47H-carrying cells suggests that either the R47H mutation causes an additional effect to the knockdown or the microglia expressing decreased *Trem2* levels throughout life *in vivo* may, once cultured outside the brain, be more prone to becoming pro-inflammatory. Either way the microglia from the R47H *Trem2* KI mice are able to respond to the pro-inflammatory LPS stimulus similarly to the WT mice or to mice with RNAi-induced knockdown, but may also show a slightly enhanced pro-inflammatory response for some markers.

In terms of genes that are induced by the IL4 anti-inflammatory stimulus, results were again generally similar to the effect of RNAi-induced knockdown. *Arg1* expression was strongly increased by IL4 treatment and the decreased *Trem2* expression in the microglia from *Trem2* R47H KI mice significantly prevented this change in a gene dose-dependent manner (Figure 9c, one-way ANOVA: main effect of genotype $p=0.002$, Sidak's multiple comparisons: $p=0.08$ for WT versus heterozygous, and $p=0.01$ for WT versus homozygous). The other anti-inflammatory marker *Tgfb1* was significantly decreased in homozygous *Trem2* R47H microglia independent of IL4-treatment, and the fold-change in *Tgfb1* up-regulation in response to treatment was similar for WT and homozygous R47H cells. These findings suggest that separate

bioRxiv preprint first posted online Oct. 22, 2018; doi: http://dx.doi.org/10.1101/449884. The copyright holder for this preprint (which was not peer-reviewed) is the author/funder, who has granted bioRxiv a license to display the preprint in perpetuity. All rights reserved. No reuse allowed without permission.

mechanisms regulate basal levels of some genes like *Tgfb1* (which may be *Trem2*-dependent at least in part), compared to mechanisms that regulate levels following induction (which can be *Trem2*-independent). Overall, the LPS-induced pro-inflammatory response was largely unaffected in the microglia carrying *Trem2* R47H alleles, but some aspects of the anti-inflammatory response to IL4 showed strong impairment with decreased *Trem2* expression, consistent between the *Trem2* knockdown and knock-in experiments.

Similarly to the *Trem2* knockdown experiments, other genes for which expression was increased in response to IL4 in, such as *Igf1, Cd68 and C1qa,* showed decreased expression in the homozygous *Trem2* R47H microglia, regardless of IL4-treatment (Figure 10; two-way ANOVA: main effect of IL4-treatment, and main effect of *Trem2* genotype, but no interaction for *Igf1*, *Cd68* and *C1qa*). As with the RNAi experiments, LPS decreased the expression of *Igf1*, *Cd68* and *C1qa*. As above, all expression data was normalized to *Rps28.* Next we saw that *Aif1* expression was also decreased in the homozygous R47H microglia relative to both WT and heterozygous R47H cells as in our knockdown experiments above (Figure 10). Note the heterozygous R47H microglia showed no changes in *Aif1* levels despite a significant reduction in *Trem2* expression suggesting this effect requires a certain threshold of knockdown. Expression of *Csf1r* and *Plcg2* were also both significantly decreased in the microglia from the *Trem2* R47H KI mice. However, for these genes the effect of genotype was already apparent in the cells from heterozygous R47H KI mice, independent of the presence of IL4 or LPS (Figure 10; two-way ANOVA: main effect of treatment, and main effect of *Trem2* genotype, but no interaction for *Csf1r* and *Plcg2*). Similarly to the siRNA knockdown experiments and in contrast to *Igf1*, *Cd68* and *C1qa*, expression of *Csf1r* was not affected by IL4, but was decreased by LPS (Figure 10; two-way ANOVA: main effect of LPS-treatment, and main effect of *Trem2* genotype, no interaction). In the case of *Plcg2*, the IL4 treatment caused a small but significant decrease in *Plcg2* expression compared to controls which was not evident in the knockdown experiment (two-way ANOVA: main effect of IL4-treatment, and main effect of *Trem2* genotype, no

bioRxiv preprint first posted online Oct. 22, 2018; doi: http://dx.doi.org/10.1101/449884. The copyright holder for this preprint (which was not peer-reviewed) is the author/funder, who has granted bioRxiv a license to display the preprint in perpetuity. All rights reserved. No reuse allowed without permission.

interaction). Unlike all the other genes tested, *Plcg2* expression was increased by LPS (two-way ANOVA: main effect of LPS-treatment, and main effect of *Trem2* genotype, no interaction). These findings confirm that decreased expression of *Trem2* in the R47H KI mice, similarly to the siRNA knockdown model, tend to make *Trem2* less effective in pushing the microglia to an anti-inflammatory phenotype compared to wild-type *Trem2*. While this is mostly because of a decrease in expression of *Trem2*, some additional mutation-specific effects may enhance the pro-inflammatory phenotype, with *Tnf* being a particular case in point.

bioRxiv preprint first posted online Oct. 22, 2018; doi: http://dx.doi.org/10.1101/449884. The copyright holder for this preprint (which was not peer-reviewed) is the author/funder, who has granted bioRxiv a license to display the preprint in perpetuity. All rights reserved. No reuse allowed without permission.

4. Discussion

4.1. *Trem2* R47H knock-in mice can largely be considered a model of *in vivo Trem2* down-regulation

Of the many genes that have been revealed in GWAS to increase the risk of AD, variants of *TREM2* have high odds ratios. The most common of these is the R47H mutation. We thus aimed to investigate the effect of this mutation in *Trem2* R47H KI mice. However in the present study we find that the primary phenotype of these mice both in primary microglial cultures and in brain tissue is a substantial gene-dose-dependent decrease in the expression of *Trem2* compared to WT mice. This effect has recently been described by Cheng-Hathaway et al. (2018) and Xiang et al. (2018) studying the same mouse line used here from the Jackson Laboratory, and an independent *Trem2* R47H KI mouse line. This does not occur in human tissue with this mutation but appears to be a mouse specific effect related to altered splicing. Hence we can largely consider these mice as a model of *Trem2* down-regulation allowing us to validate our siRNA data in primary microglia and investigate the effect of *Trem2* down-regulation *in vivo*. Any differences between the siRNA and *Trem2* R47H KI data may give initial clues to the effect of the mutation but this could also be due to the difference between expression throughout life *in vivo* versus acute transfection of the cells with siRNA. By investigating microglial density in fixed brains from the *Trem2* R47H mice, we saw a decrease in the density of microglia *in vivo* in the hippocampus, and that the remaining microglia had dramatically reduced CD68 protein levels. This raises the question as to whether any other changes that we found in *Trem2* R47H microglia are directly due to the mutation itself or downstream of its effect on impairing *Trem2* expression, and so we studied in parallel the effect of *Trem2* knockdown using siRNA in primary microglia and compared this to the *Trem2* R47H KI mouse phenotype.

bioRxiv preprint first posted online Oct. 22, 2018; doi: http://dx.doi.org/10.1101/449884. The copyright holder for this preprint (which was not peer-reviewed) is the author/funder, who has granted bioRxiv a license to display the preprint in perpetuity. All rights reserved. No reuse allowed without permission.

4.2. siRNA-induced knockdown of *Trem2* largely mimics the *Trem2* R47H phenotype in non-stimulated conditions

Knockdown of *Trem2* in the primary microglia transfected with siRNA showed similar effects to those seen in microglia from the *Trem2* R47H KI mice. In both preparations *Csf1r* expression was decreased. Pharmacological blockade of CSF1 receptors has been shown to impair microglial survival and can completely remove microglia from the mouse brain (Dagher et al. 2015; Elmore et al. 2014; Olmos-Alonso et al. 2016). These findings together with the decreased density of microglia in the hippocampus of *Trem2* R47H mice, makes it likely that the decrease in *Csf1r* expression in the microglia with decreased *Trem2* expression contributes to reduced survival of microglia. The knockdown of *Trem2* decreasing survival or altering the metabolism of microglia is consistent with previous studies (Ulland et al. 2017; Wang et al. 2015; Wu et al. 2015; Zheng et al. 2017). Interestingly no difference in *Csf1r* expression was seen in the remaining microglia in the brain tissue from the young adult KI mice, possibly suggesting different populations of microglia with loss of those more vulnerable to the effects of *Trem2* knockdown than others, at least in whole tissue. Differences in gene expression profiles of different microglial populations have been recently described using single cell RNA-seq (Hammond et al. 2018; Keren-Shaul et al. 2017).

Igf1 expression was also decreased when *Trem2* expression was knocked-down or if the *Trem2* R47H variant was carried by the primary microglial cultures. *Igf1* is abundantly expressed by microglia during postnatal development, aging, or following brain injuries and plays a vital role in promoting neuronal survival (Fernandez and Torres-Aleman 2012; Kohman et al. 2012; Thored et al. 2009; Ueno et al. 2013). While this may not affect microglial survival as the IGF1 receptor is found largely on neurons, it could contribute to neurodegeneration, being an important factor in neuronal survival and lifespan across many species (Broughton and Partridge 2009). These findings, in line with previous studies (Arkins et al. 1995; Barrett et al. 2015; Suh et al. 2013; Wynes and Riches 2003), show that *Igf1* expression is inhibited by pro-inflammatory stimuli and enhanced in anti-inflammatory

bioRxiv preprint first posted online Oct. 22, 2018; doi: http://dx.doi.org/10.1101/449884. The copyright holder for this preprint (which was not peer-reviewed) is the author/funder, who has granted bioRxiv a license to display the preprint in perpetuity. All rights reserved. No reuse allowed without permission.

environments. Thus, the *Igf1* expression decrease caused by *Trem2* deficiency may suggest a microglial phenotype shift towards pro-inflammatory activation and away from non-inflammatory, and a decrease of the pro-survival role of IGF1 on neurons. In both the human disease and in transgenic mouse models of AD, microglia have greatly increased levels of *Trem2* (Cheng-Hathaway et al. 2018; Jay et al. 2015; Lue et al. 2015; Ma et al. 2016; Melchior et al. 2010; Song et al. 2018) and this is strongly correlated with plaque load (Matarin et al. 2015). It has been reported that the microglia specifically clustering around the plaques and associated with AD have considerably higher *Igf1* expression than those distant from plaques (Kamphuis et al. 2012; Keren-Shaul et al. 2017), and the present data confirm that this is likely an effect of the higher *Trem2* expression.

4.3. *Trem2* knockdown decreases the effects of the anti-inflammatory stimulus IL4 by decreasing levels of the transcription factor STAT6

In this study we have further investigated the role of TREM2 and effects on *Trem2* expression in microglia polarized to anti-inflammatory or pro-inflammatory phenotypes. Our results suggest that there is cross-talk between the TREM2 and anti-inflammatory IL4 signaling pathways, in that TREM2 knockdown decreases levels of the STAT6 transcription factor, which is downstream of IL4 (Ohmori and Hamilton 2000). As the IL4-induced *Arg1* up-regulation is critically dependent on phosphorylation of STAT6 (Gray et al. 2005), this thus suggests that TREM2 signaling functions in parallel to support IL4-induced STAT6-gene transcription by supporting overall levels of STAT6. Decreased *Trem2* expression in both primary microglia models resulted in a decrease in IL4-induced *Arg1* expression.

ARG1 is an important anti-inflammatory marker induced upon IL4 stimulation. ARG1 in myeloid cells mainly functions as an enzyme to hydrolyze arginine to produce ornithine, which both promotes tissue repair through generation of polyamines and collagens, and also reduces nitric oxide production from inducible nitric oxide synthase through decreasing intracellular arginine availability (Mills et al. 2000; Modolell et al. 1995; Yang and Ming 2014). Our

bioRxiv preprint first posted online Oct. 22, 2018; doi: http://dx.doi.org/10.1101/449884. The copyright holder for this preprint (which was not peer-reviewed) is the author/funder, who has granted bioRxiv a license to display the preprint in perpetuity. All rights reserved. No reuse allowed without permission.

findings in cultured primary microglia suggest an attenuated anti-inflammatory phenotype with reduced expression of *Trem2*, with both the RNAi and the *Trem2* R47H mutation substantially inhibiting this IL4-induced microglial response (Figure 11).

It has also been suggested in macrophages that STAT6 is essential for IL4-mediated up-regulation of *Igf1* expression (Wynes and Riches 2003). While there is a decrease in *Igf1* expression in the cultured microglia in this present study, this is independent of IL4, occurring also under control conditions when *Trem2* is knocked down. Therefore, it is possible that the decrease in *Igf1* in the *Trem2*-deficient microglia results from decreased STAT6 levels.

In hippocampal homogenates from young adult *Trem2* R47H mice, we did not see differences in expression of the genes we studied, including *Stat6* and *Igf1*, despite a slight but significant reduction in the number of microglia. Lack of gene expression changes *in vivo* may be due to a supportive environment from healthy neurons and astrocytes, providing regulating input to the microglia in young mice. Other studies have not revealed obvious phenotypes in young *Trem2* R47H expressing mice, or even *Trem2* knockout mice, unless they are bred to amyloid mouse models (Song et al. 2018), and so future studies need to characterize these pathways in *Trem2* R47H mice crossed with amyloid models, or in aged mice. The effects seen in the primary cultured microglia probably reflect a different mean activation state from microglia in the brain environment. However the pathway interactions described here between *Trem2* expression and other genes, in primary microglial cultures, nevertheless reflects effects that *Trem2* can have under particular conditions. This also applies to the relationship between *Trem2* expression and the IL4-induction of *Arg1* expression putatively via STAT6.

bioRxiv preprint first posted online Oct. 22, 2018; doi: http://dx.doi.org/10.1101/449884. The copyright holder for this preprint (which was not peer-reviewed) is the author/funder, who has granted bioRxiv a license to display the preprint in perpetuity. All rights reserved. No reuse allowed without permission.

4.4. Pro-inflammatory stimuli prevent the effects of TREM2 by inhibiting its expression, similar to the effect seen in microglia from *Trem2* R47H KI mice

With LPS stimulation, primary microglia from WT mice exhibited a robust pro-inflammatory response in microglia, as measured by strong up-regulation of *Tnf* and *Il1b* expression (Figure 11). In contrast IL4 stimulation had little effect on *Trem2* expression. In agreement with previous findings (Owens et al. 2017), LPS largely suppressed *Trem2* expression with a decrease in expression beginning as early as 3 hr after LPS application and reaching more than an 85% decrease by 24 hr. This finding is consistent with previous studies showing that LPS/IFNγ stimulation down-regulated *Trem2* expression via TLR4 receptors in cell lines and primary cultures of microglia/macrophages and also in mouse brains (Owens et al. 2017; Schmid et al. 2002; Turnbull et al. 2006; Zheng et al. 2016). Moreover, Owens and colleagues (2017) showed that treatment with pro-inflammatory mediators engaging other Toll-like receptors (TLRs) also suppressed *Trem2* expression in the BV-2 cell line, albeit with slightly different potency. This suggests that the *Trem2* down-regulation is not specific to LPS-TLR4 signaling but perhaps a common event occurring in microglial induced by various classical pro-inflammatory stimuli. While, under conditions of *Trem2* knockdown, the levels of expression were even lower after 24 hr exposure to LPS, it is not surprising that this additional knockdown had little effect on the expression of LPS-induced gene expression as so little *Trem2* expression remained, even in the control microglia. Hence, in conditions of *Trem2* knockdown, very similar LPS-induced up-regulation of *Tnf* and *Il1b* expression resulted. It was interesting to note however that in the microglia originating from *Trem2* R47H KI mice with a similar level of *Trem2* down-regulation that there was about a 30% increase in the activation of *Tnf* compared to WT mice possibly suggesting that the *Trem2* R47H mutation further enhances this effect. There are other possible explanations for this difference however as the down-regulation of *Trem2* in these mice is present throughout life and so these microglia may have a different state when isolated than those in which *Trem2* is knocked down acutely.

bioRxiv preprint first posted online Oct. 22, 2018; doi: http://dx.doi.org/10.1101/449884. The copyright holder for this preprint (which was not peer-reviewed) is the author/funder, who has granted bioRxiv a license to display the preprint in perpetuity. All rights reserved. No reuse allowed without permission.

It has been suggested that the SPI1 transcription factor (PU.1) is responsible for transcription of *Trem2*, at least in the BV-2 cell line (Huang et al. 2017; Satoh et al. 2014), but in our primary microglia, LPS significantly increased the expression of *Spi1*, whereas *Trem2* expression was strongly suppressed suggesting that, at least in this context, factors other than SPI1 also regulate *Trem2* expression.

Taken together, pro-inflammatory mediators, either locally produced or infiltrating into the CNS from the periphery, could induce down-regulation of microglial *Trem2* expression and subsequently induce a microglial state with low TREM2-signaling (Figure 11). This might reflect a mechanism for microglia to perform specific functional requirements under pro-inflammatory conditions. Although, accumulated pro-inflammation and oxidative stress in the brain, which is often observed in aged brains and aged microglia (Godbout et al. 2005; Lee et al. 2000; Prolla 2002; Sierra et al. 2007; Verbitsky et al. 2004), could cause sustained suppression of *Trem2* expression and thus an impairment of TREM2-dependent microglial functions. This might be one of the major mechanisms underlying TREM2 dysfunction that contributes to sporadic AD progression with advanced age, since *TREM2* variants associated with increased AD risk are extremely rare in frequency in humans (Guerreiro et al. 2013b). It is, however, important to note that, in conditions of decreased *Trem2* expression in the *Trem2* R47H KI mice, the number of IBA1-positive mouse microglia was decreased in hippocampal sections. However, when *Trem2* was almost completely inhibited by the pro-inflammatory stimulus, this does not result in obvious changes in *Aif1* expression, suggesting that under these conditions additional factors control *Aif1* expression in individual microglia and this could prevent a loss of microglia from undermining the pro-inflammatory response. Moreover increased *Trem2* expression as occurs in Alzheimer's disease (Cheng-Hathaway et al. 2018; Jay et al. 2015; Lue et al. 2015; Ma et al. 2016; Melchior et al. 2010; Song et al. 2018) could protect the brain from the damaging effects of inflammation.

bioRxiv preprint first posted online Oct. 22, 2018; doi: http://dx.doi.org/10.1101/449884. The copyright holder for this preprint (which was not peer-reviewed) is the author/funder, who has granted bioRxiv a license to display the preprint in perpetuity. All rights reserved. No reuse allowed without permission.

4.5. Functions of TREM2 in Alzheimer's disease and the effect of the R47H mutation

Recent important studies have also shown that the R47H variant of *Trem2* acts by loss-of-function and impairs the microglial response to amyloid pathology by regulating microglial number around plaques and microglial activity, but anti-inflammatory signaling was not studied (Cheng-Hathaway et al. 2018; Song et al. 2018). Thus, an important issue about microglial activation *in vivo* has to be carefully considered: in contrast to populations of microglia polarized with purified LPS or IL4 stimuli *in vitro*, microglia *in vivo* probably never receive such simple stimuli to govern their activation status or at least not across the whole population. Instead, they are modulated by mixed cues including various regulatory signals from the local environment (*e.g.* from neurons and astrocytes), which could possibly lead to a more mixed, dynamic and context-dependent microglial phenotype *in vivo*. There is increasing evidence that reactive microglia in diseased brains demonstrate a mixed phenotype with expression of both pro- and anti-inflammatory markers, even at the single-cell level, rather than completely reproducing the phenotype obtained from homogenous *in vitro* polarization studies (Chiu et al. 2013; Holtman et al. 2015; Kim et al. 2016; Morganti et al. 2016). Indeed, a recent study identified a unique transcriptional signature in phagocytic microglia associated with amyloid plaques, which was in part dependent on *Trem2* and included *Igf1* and *Csf1* (Keren-Shaul et al. 2017). Therefore, we are cautious in directly applying the *in vitro* phenotype to interpretation of *in vivo* microglial activation. However, we propose pro- and anti-inflammatory stimuli still represent an important part of the driving factors determining where in the entire multidimensional continuum of microglial activation microglia fall and understanding their effects separately and without the influence of other cell types may help to differentiate possible methods for moderating function in disease.

Thus, to study the relevance of TREM2 in regulating microglial activation, we used the polarization experiments to dissect the reaction of microglia in response to either pro- or anti-inflammatory stimuli and investigate the effects

bioRxiv preprint first posted online Oct. 22, 2018; doi: http://dx.doi.org/10.1101/449884. The copyright holder for this preprint (which was not peer-reviewed) is the author/funder, who has granted bioRxiv a license to display the preprint in perpetuity. All rights reserved. No reuse allowed without permission.

of *Trem2* deficiency in each direction. Overall, our data shows that decreased expression of *Trem2* has acute and chronic effects on a subset of non-inflammatory functions in microglial cells that overlap with IL4 anti-inflammatory signaling (Figure 11). Moreover, *Trem2* seems to support the survival of microglia at least in part via expression of the *Csf1r*. Interestingly, when we tested expression of genes that show substantial changes in transgenic mice associated with AD (Matarin et al. 2015) a number of aspects of gene expression were mimicked by anti-inflammatory IL4 stimulation, whereas the pro-inflammatory effects of LPS had the opposite effect, leading to almost complete down-regulation of *Trem2* expression. This suggests that the very strong microglial response to plaque deposition that we have previously reported in transgenic mice (Matarin et al. 2015), particularly the up to 6-fold increase in *Trem2* expression, is a protective anti-inflammatory response that may contribute to the resistance of mice with a heavy amyloid load from developing the full AD pathology of Tau tangles and neurodegeneration. The balance of anti-inflammatory and pro-inflammatory phenotype is very likely related to the balance between microglia protecting against or exacerbating the progression of AD. Generally, *Trem2* seems to enhance the anti-inflammatory phenotype protecting against disease progression and moreover may increase the number of protective microglia. Pro-inflammatory stimuli inhibit this effect by down-regulating the expression of *Trem2*. Although in this study, the down-regulation of *Trem2* expression in the *Trem2* R47H KI mice which is not reflected in humans with this mutation, means that we can conclude little about the effect of the R47H mutation itself, this is nevertheless a model for loss of function of *Trem2* and validates our findings on the effects of siRNA-induced knockdown. Our findings are thus compatible with increased expression of *TREM2* in Alzheimer's disease having a protective function slowing disease progression and hence loss of function due to the presence of the *Trem2* R47H mutation increasing the chance of AD reaching the stage of diagnosis. Further work into the molecular pathways regulated by TREM2, particularly the cross-talk with anti-inflammatory pathways, may provide important insights for therapeutic approaches.

bioRxiv preprint first posted online Oct. 22, 2018; doi: http://dx.doi.org/10.1101/449884. The copyright holder for this preprint (which was not peer-reviewed) is the author/funder, who has granted bioRxiv a license to display the preprint in perpetuity. All rights reserved. No reuse allowed without permission.

References

Arkins S, Rebeiz N, Brunke-Reese DL, Biragyn A, Kelley KW. 1995. Interferon-gamma inhibits macrophage insulin-like growth factor-I synthesis at the transcriptional level. Mol Endocrinol 9:350-60.

Atagi Y, Liu CC, Painter MM, Chen XF, Verbeeck C, Zheng H, Li X, Rademakers R, Kang SS, Xu H and others. 2015. Apolipoprotein E Is a Ligand for Triggering Receptor Expressed on Myeloid Cells 2 (TREM2). J Biol Chem 290:26043-50.

Barrett JP, Minogue AM, Falvey A, Lynch MA. 2015. Involvement of IGF-1 and Akt in M1/M2 activation state in bone marrow-derived macrophages. Exp Cell Res 335:258-68.

Benitez BA, Cruchaga C, United States-Spain Parkinson's Disease Research G. 2013. TREM2 and neurodegenerative disease. N Engl J Med 369:1567-8.

Bouchon A, Dietrich J, Colonna M. 2000. Cutting edge: inflammatory responses can be triggered by TREM-1, a novel receptor expressed on neutrophils and monocytes. J Immunol 164:4991-5.

Bouchon A, Hernandez-Munain C, Cella M, Colonna M. 2001. A DAP12-mediated pathway regulates expression of CC chemokine receptor 7 and maturation of human dendritic cells. J Exp Med 194:1111-22.

Broughton S, Partridge L. 2009. Insulin/IGF-like signalling, the central nervous system and aging. Biochem J 418:1-12.

Cady J, Koval ED, Benitez BA, Zaidman C, Jockel-Balsarotti J, Allred P, Baloh RH, Ravits J, Simpson E, Appel SH and others. 2014. TREM2 variant p.R47H as a risk factor for sporadic amyotrophic lateral sclerosis. JAMA Neurol 71:449-53.

Cheng-Hathaway PJ, Reed-Geaghan EG, Jay TR, Casali BT, Bemiller SM, Puntambekar SS, von Saucken VE, Williams RY, Karlo JC, Moutinho M and others. 2018. The Trem2 R47H variant confers loss-of-function-like phenotypes in Alzheimer's disease. Mol Neurodegener 13:29.

Chiu IM, Morimoto ET, Goodarzi H, Liao JT, O'Keeffe S, Phatnani HP, Muratet M, Carroll MC, Levy S, Tavazoie S and others. 2013. A neurodegeneration-specific gene-expression signature of acutely isolated microglia from an amyotrophic lateral sclerosis mouse model. Cell Rep 4:385-401.

Dagher NN, Najafi AR, Kayala KM, Elmore MR, White TE, Medeiros R, West BL, Green KN. 2015. Colony-stimulating factor 1 receptor inhibition prevents microglial plaque association and improves cognition in 3xTg-AD mice. J Neuroinflammation 12:139.

Daws MR, Lanier LL, Seaman WE, Ryan JC. 2001. Cloning and characterization of a novel mouse myeloid DAP12-associated receptor family. Eur J Immunol 31:783-91.

Elmore MR, Najafi AR, Koike MA, Dagher NN, Spangenberg EE, Rice RA, Kitazawa M, Matusow B, Nguyen H, West BL and others. 2014. Colony-stimulating factor 1 receptor signaling is necessary for microglia viability, unmasking a microglia progenitor cell in the adult brain. Neuron 82:380-97.

bioRxiv preprint first posted online Oct. 22, 2018; doi: http://dx.doi.org/10.1101/449884. The copyright holder for this preprint (which was not peer-reviewed) is the author/funder, who has granted bioRxiv a license to display the preprint in perpetuity. All rights reserved. No reuse allowed without permission.

Fernandez AM, Torres-Aleman I. 2012. The many faces of insulin-like peptide signalling in the brain. Nat Rev Neurosci 13:225-39.

Gao X, Dong Y, Liu Z, Niu B. 2013. Silencing of triggering receptor expressed on myeloid cells-2 enhances the inflammatory responses of alveolar macrophages to lipopolysaccharide. Mol Med Rep 7:921-6.

Garcia-Reitboeck P, Phillips A, Piers TM, Villegas-Llerena C, Butler MG, Mallach A, Rodrigues C, Arber CE, Heslegrave A, Zetterberg H and others. 2018. Human induced pluripotent stem cell-derived microglia-like cells harboring TREM2 missense mutations show specific deficits in phagocytosis. Cell Reports 24:2300-2311.

Ginhoux F, Greter M, Leboeuf M, Nandi S, See P, Gokhan S, Mehler MF, Conway SJ, Ng LG, Stanley ER and others. 2010. Fate mapping analysis reveals that adult microglia derive from primitive macrophages. Science 330:841-5.

Godbout JP, Chen J, Abraham J, Richwine AF, Berg BM, Kelley KW, Johnson RW. 2005. Exaggerated neuroinflammation and sickness behavior in aged mice following activation of the peripheral innate immune system. FASEB J 19:1329-31.

Gordon S, Martinez FO. 2010. Alternative activation of macrophages: mechanism and functions. Immunity 32:593-604.

Gray MJ, Poljakovic M, Kepka-Lenhart D, Morris SM, Jr. 2005. Induction of arginase I transcription by IL-4 requires a composite DNA response element for STAT6 and C/EBPbeta. Gene 353:98-106.

Griciuc A, Serrano-Pozo A, Parrado AR, Lesinski AN, Asselin CN, Mullin K, Hooli B, Choi SH, Hyman BT, Tanzi RE. 2013. Alzheimer's disease risk gene CD33 inhibits microglial uptake of amyloid beta. Neuron 78:631-43.

Guerreiro R, Bilgic B, Guven G, Bras J, Rohrer J, Lohmann E, Hanagasi H, Gurvit H, Emre M. 2013a. Novel compound heterozygous mutation in TREM2 found in a Turkish frontotemporal dementia-like family. Neurobiol Aging 34:2890 e1-5.

Guerreiro R, Wojtas A, Bras J, Carrasquillo M, Rogaeva E, Majounie E, Cruchaga C, Sassi C, Kauwe JS, Younkin S and others. 2013b. TREM2 variants in Alzheimer's disease. N Engl J Med 368:117-27.

Guerreiro RJ, Lohmann E, Bras JM, Gibbs JR, Rohrer JD, Gurunlian N, Dursun B, Bilgic B, Hanagasi H, Gurvit H and others. 2013c. Using exome sequencing to reveal mutations in TREM2 presenting as a frontotemporal dementia-like syndrome without bone involvement. JAMA Neurol 70:78-84.

Hammond TR, Dufort C, Dissing-Olesen L, Giera S, Young A, Wysoker A, Walker AJ, Segel M, Nemesh J, Saunders A and others. 2018. Complex cell-state changes revealed by single cell RNA sequencing of 76,149 microglia throughout the mouse lifespan and in the injured brain. bioRxiv. doi: 10.1101/406140.

Hollingworth P, Harold D, Sims R, Gerrish A, Lambert JC, Carrasquillo MM, Abraham R, Hamshere ML, Pahwa JS, Moskvina V and others. 2011. Common variants at ABCA7, MS4A6A/MS4A4E, EPHA1, CD33 and CD2AP are associated with Alzheimer's disease. Nat Genet 43:429-35.

bioRxiv preprint first posted online Oct. 22, 2018; doi: http://dx.doi.org/10.1101/449884. The copyright holder for this preprint (which was not peer-reviewed) is the author/funder, who has granted bioRxiv a license to display the preprint in perpetuity. All rights reserved. No reuse allowed without permission.

Holness CL, Simmons DL. 1993. Molecular cloning of CD68, a human macrophage marker related to lysosomal glycoproteins. Blood 81:1607-13.

Holtman IR, Raj DD, Miller JA, Schaafsma W, Yin Z, Brouwer N, Wes PD, Moller T, Orre M, Kamphuis W and others. 2015. Induction of a common microglia gene expression signature by aging and neurodegenerative conditions: a co-expression meta-analysis. Acta Neuropathol Commun 3:31.

Huang KL, Marcora E, Pimenova AA, Di Narzo AF, Kapoor M, Jin SC, Harari O, Bertelsen S, Fairfax BP, Czajkowski J and others. 2017. A common haplotype lowers PU.1 expression in myeloid cells and delays onset of Alzheimer's disease. Nat Neurosci 20:1052-1061.

Humphrey MB, Daws MR, Spusta SC, Niemi EC, Torchia JA, Lanier LL, Seaman WE, Nakamura MC. 2006. TREM2, a DAP12-associated receptor, regulates osteoclast differentiation and function. J Bone Miner Res 21:237-45.

Jay TR, Miller CM, Cheng PJ, Graham LC, Bemiller S, Broihier ML, Xu G, Margevicius D, Karlo JC, Sousa GL and others. 2015. TREM2 deficiency eliminates TREM2+ inflammatory macrophages and ameliorates pathology in Alzheimer's disease mouse models. J Exp Med 212:287-95.

Jiang T, Tan L, Chen Q, Tan MS, Zhou JS, Zhu XC, Lu H, Wang HF, Zhang YD, Yu JT. 2016. A rare coding variant in TREM2 increases risk for Alzheimer's disease in Han Chinese. Neurobiol Aging 42:217 e1-3.

Jin SC, Benitez BA, Karch CM, Cooper B, Skorupa T, Carrell D, Norton JB, Hsu S, Harari O, Cai Y and others. 2014. Coding variants in TREM2 increase risk for Alzheimer's disease. Hum Mol Genet 23:5838-46.

Jonsson T, Stefansson H, Steinberg S, Jonsdottir I, Jonsson PV, Snaedal J, Bjornsson S, Huttenlocher J, Levey AI, Lah JJ and others. 2013. Variant of TREM2 associated with the risk of Alzheimer's disease. N Engl J Med 368:107-16.

Kamphuis W, Orre M, Kooijman L, Dahmen M, Hol EM. 2012. Differential cell proliferation in the cortex of the APPswePS1dE9 Alzheimer's disease mouse model. Glia 60:615-29.

Keren-Shaul H, Spinrad A, Weiner A, Matcovitch-Natan O, Dvir-Szternfeld R, Ulland TK, David E, Baruch K, Lara-Astaiso D, Toth B and others. 2017. A Unique Microglia Type Associated with Restricting Development of Alzheimer's Disease. Cell 169:1276-1290 e17.

Kim CC, Nakamura MC, Hsieh CL. 2016. Brain trauma elicits non-canonical macrophage activation states. J Neuroinflammation 13:117.

Kleinberger G, Yamanishi Y, Suarez-Calvet M, Czirr E, Lohmann E, Cuyvers E, Struyfs H, Pettkus N, Wenninger-Weinzierl A, Mazaheri F and others. 2014. TREM2 mutations implicated in neurodegeneration impair cell surface transport and phagocytosis. Sci Transl Med 6:243ra86.

Kohman RA, DeYoung EK, Bhattacharya TK, Peterson LN, Rhodes JS. 2012. Wheel running attenuates microglia proliferation and increases expression of a proneurogenic phenotype in the hippocampus of aged mice. Brain Behav Immun 26:803-10.

bioRxiv preprint first posted online Oct. 22, 2018; doi: http://dx.doi.org/10.1101/449884. The copyright holder for this preprint (which was not peer-reviewed) is the author/funder, who has granted bioRxiv a license to display the preprint in perpetuity. All rights reserved. No reuse allowed without permission.

Lee CK, Weindruch R, Prolla TA. 2000. Gene-expression profile of the ageing brain in mice. Nat Genet 25:294-7.

Lue LF, Schmitz CT, Serrano G, Sue LI, Beach TG, Walker DG. 2015. TREM2 Protein Expression Changes Correlate with Alzheimer's Disease Neurodegenerative Pathologies in Post-Mortem Temporal Cortices. Brain Pathol 25:469-80.

Luzina IG, Keegan AD, Heller NM, Rook GA, Shea-Donohue T, Atamas SP. 2012. Regulation of inflammation by interleukin-4: a review of "alternatives". J Leukoc Biol 92:753-64.

Ma L, Allen M, Sakae N, Ertekin-Taner N, Graff-Radford NR, Dickson DW, Younkin SG, Sevlever D. 2016. Expression and processing analyses of wild type and p.R47H TREM2 variant in Alzheimer's disease brains. Mol Neurodegener 11:72.

Malik M, Simpson JF, Parikh I, Wilfred BR, Fardo DW, Nelson PT, Estus S. 2013. CD33 Alzheimer's risk-altering polymorphism, CD33 expression, and exon 2 splicing. J Neurosci 33:13320-5.

Matarin M, Salih DA, Yasvoina M, Cummings DM, Guelfi S, Liu W, Nahaboo Solim MA, Moens TG, Paublete RM, Ali SS and others. 2015. A genome-wide gene-expression analysis and database in transgenic mice during development of amyloid or tau pathology. Cell Rep 10:633-44.

Melchior B, Garcia AE, Hsiung BK, Lo KM, Doose JM, Thrash JC, Stalder AK, Staufenbiel M, Neumann H, Carson MJ. 2010. Dual induction of TREM2 and tolerance-related transcript, Tmem176b, in amyloid transgenic mice: implications for vaccine-based therapies for Alzheimer's disease. ASN Neuro 2:e00037.

Mills CD, Kincaid K, Alt JM, Heilman MJ, Hill AM. 2000. M-1/M-2 macrophages and the Th1/Th2 paradigm. J Immunol 164:6166-73.

Modolell M, Corraliza IM, Link F, Soler G, Eichmann K. 1995. Reciprocal regulation of the nitric oxide synthase/arginase balance in mouse bone marrow-derived macrophages by TH1 and TH2 cytokines. Eur J Immunol 25:1101-4.

Morganti JM, Riparip LK, Rosi S. 2016. Call Off the Dog(ma): M1/M2 Polarization Is Concurrent following Traumatic Brain Injury. PLoS One 11:e0148001.

Murray CE, King A, Troakes C, Hodges A, Lashley T. 2018. APOE epsilon4 is also required in TREM2 R47H variant carriers for Alzheimer's disease to develop. Neuropathol Appl Neurobiol. doi: 10.1111/nan.12474.

Naj AC, Jun G, Beecham GW, Wang LS, Vardarajan BN, Buros J, Gallins PJ, Buxbaum JD, Jarvik GP, Crane PK and others. 2011. Common variants at MS4A4/MS4A6E, CD2AP, CD33 and EPHA1 are associated with late-onset Alzheimer's disease. Nat Genet 43:436-41.

Nelms K, Keegan AD, Zamorano J, Ryan JJ, Paul WE. 1999. The IL-4 receptor: signaling mechanisms and biologic functions. Annu Rev Immunol 17:701-38.

Ohmori Y, Hamilton TA. 2000. Interleukin-4/STAT6 represses STAT1 and NF-kappa B-dependent transcription through distinct mechanisms. J Biol Chem 275:38095-103.

bioRxiv preprint first posted online Oct. 22, 2018; doi: http://dx.doi.org/10.1101/449884. The copyright holder for this preprint (which was not peer-reviewed) is the author/funder, who has granted bioRxiv a license to display the preprint in perpetuity. All rights reserved. No reuse allowed without permission.

Ohsawa K, Imai Y, Kanazawa H, Sasaki Y, Kohsaka S. 2000. Involvement of Iba1 in membrane ruffling and phagocytosis of macrophages/microglia. J Cell Sci 113 (Pt 17):3073-84.

Olmos-Alonso A, Schetters ST, Sri S, Askew K, Mancuso R, Vargas-Caballero M, Holscher C, Perry VH, Gomez-Nicola D. 2016. Pharmacological targeting of CSF1R inhibits microglial proliferation and prevents the progression of Alzheimer's-like pathology. Brain 139(Pt3):891-907.

Owens R, Grabert K, Davies CL, Alfieri A, Antel JP, Healy LM, McColl BW. 2017. Divergent Neuroinflammatory Regulation of Microglial TREM Expression and Involvement of NF-kappaB. Front Cell Neurosci 11:56.

Paloneva J, Mandelin J, Kiialainen A, Bohling T, Prudlo J, Hakola P, Haltia M, Konttinen YT, Peltonen L. 2003. DAP12/TREM2 deficiency results in impaired osteoclast differentiation and osteoporotic features. J Exp Med 198:669-75.

Paloneva J, Manninen T, Christman G, Hovanes K, Mandelin J, Adolfsson R, Bianchin M, Bird T, Miranda R, Salmaggi A and others. 2002. Mutations in two genes encoding different subunits of a receptor signaling complex result in an identical disease phenotype. Am J Hum Genet 71:656-62.

Paradowska-Gorycka A, Jurkowska M. 2013. Structure, expression pattern and biological activity of molecular complex TREM-2/DAP12. Hum Immunol 74:730-7.

Prolla TA. 2002. DNA microarray analysis of the aging brain. Chem Senses 27:299-306.

Rayaprolu S, Mullen B, Baker M, Lynch T, Finger E, Seeley WW, Hatanpaa KJ, Lomen-Hoerth C, Kertesz A, Bigio EH and others. 2013. TREM2 in neurodegeneration: evidence for association of the p.R47H variant with frontotemporal dementia and Parkinson's disease. Mol Neurodegener 8:19.

Ruiz A, Dols-Icardo O, Bullido MJ, Pastor P, Rodriguez-Rodriguez E, Lopez de Munain A, de Pancorbo MM, Perez-Tur J, Alvarez V, Antonell A and others. 2014. Assessing the role of the TREM2 p.R47H variant as a risk factor for Alzheimer's disease and frontotemporal dementia. Neurobiol Aging 35:444 e1-4.

Saito N, Pulford KA, Breton-Gorius J, Masse JM, Mason DY, Cramer EM. 1991. Ultrastructural localization of the CD68 macrophage-associated antigen in human blood neutrophils and monocytes. Am J Pathol 139:1053-9.

Satoh J, Asahina N, Kitano S, Kino Y. 2014. A Comprehensive Profile of ChIP-Seq-Based PU.1/Spi1 Target Genes in Microglia. Gene Regul Syst Bio 8:127-39.

Saura J, Tusell JM, Serratosa J. 2003. High-yield isolation of murine microglia by mild trypsinization. Glia 44:183-9.

Schildge S, Bohrer C, Beck K, Schachtrup C. 2013. Isolation and culture of mouse cortical astrocytes. J Vis Exp 71:e50079. doi: 10.3791/50079.

Schmid CD, Sautkulis LN, Danielson PE, Cooper J, Hasel KW, Hilbush BS, Sutcliffe JG, Carson MJ. 2002. Heterogeneous expression of the triggering receptor expressed on myeloid cells-2 on adult murine microglia. J Neurochem 83:1309-20.

bioRxiv preprint first posted online Oct. 22, 2018; doi: http://dx.doi.org/10.1101/449884. The copyright holder for this preprint (which was not peer-reviewed) is the author/funder, who has granted bioRxiv a license to display the preprint in perpetuity. All rights reserved. No reuse allowed without permission.

Sierra A, Gottfried-Blackmore AC, McEwen BS, Bulloch K. 2007. Microglia derived from aging mice exhibit an altered inflammatory profile. Glia 55:412-24.

Sims R, van der Lee SJ, Naj AC, Bellenguez C, Badarinarayan N, Jakobsdottir J, Kunkle BW, Boland A, Raybould R, Bis JC and others. 2017. Rare coding variants in PLCG2, ABI3, and TREM2 implicate microglial-mediated innate immunity in Alzheimer's disease. Nat Genet 49:1373-1384.

Song WM, Joshita S, Zhou Y, Ulland TK, Gilfillan S, Colonna M. 2018. Humanized TREM2 mice reveal microglia-intrinsic and -extrinsic effects of R47H polymorphism. J Exp Med 215:745-760.

Suh HS, Zhao ML, Derico L, Choi N, Lee SC. 2013. Insulin-like growth factor 1 and 2 (IGF1, IGF2) expression in human microglia: differential regulation by inflammatory mediators. J Neuroinflammation 10:37.

Takahashi K, Rochford CD, Neumann H. 2005. Clearance of apoptotic neurons without inflammation by microglial triggering receptor expressed on myeloid cells-2. J Exp Med 201:647-57.

Thored P, Heldmann U, Gomes-Leal W, Gisler R, Darsalia V, Taneera J, Nygren JM, Jacobsen SE, Ekdahl CT, Kokaia Z and others. 2009. Long-term accumulation of microglia with proneurogenic phenotype concomitant with persistent neurogenesis in adult subventricular zone after stroke. Glia 57:835-49.

Turnbull IR, Gilfillan S, Cella M, Aoshi T, Miller M, Piccio L, Hernandez M, Colonna M. 2006. Cutting edge: TREM-2 attenuates macrophage activation. J Immunol 177:3520-4.

Ueno M, Fujita Y, Tanaka T, Nakamura Y, Kikuta J, Ishii M, Yamashita T. 2013. Layer V cortical neurons require microglial support for survival during postnatal development. Nat Neurosci 16:543-51.

Ulland TK, Song WM, Huang SC, Ulrich JD, Sergushichev A, Beatty WL, Loboda AA, Zhou Y, Cairns NJ, Kambal A and others. 2017. TREM2 Maintains Microglial Metabolic Fitness in Alzheimer's Disease. Cell 170:649-663 e13.

Verbitsky M, Yonan AL, Malleret G, Kandel ER, Gilliam TC, Pavlidis P. 2004. Altered hippocampal transcript profile accompanies an age-related spatial memory deficit in mice. Learn Mem 11:253-60.

Wang Y, Cella M, Mallinson K, Ulrich JD, Young KL, Robinette ML, Gilfillan S, Krishnan GM, Sudhakar S, Zinselmeyer BH and others. 2015. TREM2 Lipid Sensing Sustains the Microglial Response in an Alzheimer's Disease Model. Cell 160:1061-71.

Wang Y, Ulland TK, Ulrich JD, Song W, Tzaferis JA, Hole JT, Yuan P, Mahan TE, Shi Y, Gilfillan S and others. 2016. TREM2-mediated early microglial response limits diffusion and toxicity of amyloid plaques. J Exp Med 213:667-75.

Wu K, Byers DE, Jin X, Agapov E, Alexander-Brett J, Patel AC, Cella M, Gilfilan S, Colonna M, Kober DL and others. 2015. TREM-2 promotes macrophage survival and lung disease after respiratory viral infection. J Exp Med 212:681-97.

Wynes MW, Riches DW. 2003. Induction of macrophage insulin-like growth factor-I expression by the Th2 cytokines IL-4 and IL-13. J Immunol 171:3550-9.

bioRxiv preprint first posted online Oct. 22, 2018; doi: http://dx.doi.org/10.1101/449884. The copyright holder for this preprint (which was not peer-reviewed) is the author/funder, who has granted bioRxiv a license to display the preprint in perpetuity. All rights reserved. No reuse allowed without permission.

Xiang X, Piers TM, Wefers B, Zhu K, Mallach A, Brunner B, Kleinberger G, Song W, Colonna M, Herms J and others. 2018. The Trem2 R47H Alzheimer's risk variant impairs splicing and reduces Trem2 mRNA and protein in mice but not in humans. Mol Neurodegener 13:49.

Xiang X, Werner G, Bohrmann B, Liesz A, Mazaheri F, Capell A, Feederle R, Knuesel I, Kleinberger G, Haass C. 2016. TREM2 deficiency reduces the efficacy of immunotherapeutic amyloid clearance. EMBO Mol Med 8:992-1004.

Yang Z, Ming XF. 2014. Functions of arginase isoforms in macrophage inflammatory responses: impact on cardiovascular diseases and metabolic disorders. Front Immunol 5:533.

Yeh FL, Wang Y, Tom I, Gonzalez LC, Sheng M. 2016. TREM2 Binds to Apolipoproteins, Including APOE and CLU/APOJ, and Thereby Facilitates Uptake of Amyloid-Beta by Microglia. Neuron 91:328-40.

Zhao Y, Wu X, Li X, Jiang LL, Gui X, Liu Y, Sun Y, Zhu B, Pina-Crespo JC, Zhang M and others. 2018. TREM2 Is a Receptor for beta-Amyloid that Mediates Microglial Function. Neuron 97:1023-1031 e7.

Zheng H, Jia L, Liu CC, Rong Z, Zhong L, Yang L, Chen XF, Fryer JD, Wang X, Zhang YW and others. 2017. TREM2 promotes microglial survival by activating Wnt/beta-catenin pathway. J Neurosci 37:1772-1784.

Zheng H, Liu CC, Atagi Y, Chen XF, Jia L, Yang L, He W, Zhang X, Kang SS, Rosenberry TL and others. 2016. Opposing roles of the triggering receptor expressed on myeloid cells 2 and triggering receptor expressed on myeloid cells-like transcript 2 in microglia activation. Neurobiol Aging 42:132-41.

Zhong L, Chen XF, Zhang ZL, Wang Z, Shi XZ, Xu K, Zhang YW, Xu H, Bu G. 2015. DAP12 Stabilizes the C-terminal Fragment of the Triggering Receptor Expressed on Myeloid Cells-2 (TREM2) and Protects against LPS-induced Pro-inflammatory Response. J Biol Chem 290:15866-77.

bioRxiv preprint first posted online Oct. 22, 2018; doi: http://dx.doi.org/10.1101/449884. The copyright holder for this preprint (which was not peer-reviewed) is the author/funder, who has granted bioRxiv a license to display the preprint in perpetuity. All rights reserved. No reuse allowed without permission.

Figure legends

FIGURE 1. Establishing the *in vitro* primary microglial model of acute *Trem2* knockdown.

(a) Schedule of the *in vitro Trem2* knockdown experiment, and treatment with LPS or IL4. (b) Left panel: primary microglia stained with an antibody against IBA1 and DAPI. Right panel: a higher-magnification image showing the morphology of microglia *in vitro*. (c) Pro- and anti-inflammatory gene expression changes in primary microglia with either LPS or IL4 treatment. N=3-6 independent experiments. Data shown as mean ± SEM.

FIGURE 2. *Trem2* knockdown induced impaired phagocytosis in primary microglia. (a) Comparison of *Trem2* knockdown in the presence of 3 siRNA sequences vs. non-targeting siRNA in BV-2 cell cultures (N=3). The siRNA No. 2 was chosen for the following *in vitro* acute *Trem2*-knockdown experiments due to its high knockdown levels. (b) *Trem2* siRNA efficiency tested with RT-qPCR at 72 hr after transfection in primary microglia. N=13 independent cell preparations. (c) Phagocytosis assay was performed using pHrodo-conjugated *E. coli* and analyzed by FACS. As a negative control, phagocytosis was inhibited with 10 mM cytochalasin D. Left and middle panels: a representative experiment. Left panel: forward (FSC-H) versus side (SSC-H) scatter of light to allow identification of single microglial cells of the expected size and granularity (shown within the blue gate). Middle panel: frequency of microglia containing different levels of phagocytosed fluorescent bacteria. Right panel: phagocytosis in microglia with *Trem2* knockdown. N=3 independent experiments. Data shown as mean ± SEM. Paired t-test (paired within each culture preparation); * $p<0.05$, ** $p<0.01$, *** $p<0.001$, **** $p<0.0001$.

FIGURE 3. Gene expression changes in primary microglia with acute *Trem2* knockdown. The mRNA levels of individual genes at 72 hours post transfection were first normalized to *Rps28*, and then the relative fold change in the knockdown was calculated versus the negative control from the same

bioRxiv preprint first posted online Oct. 22, 2018; doi: http://dx.doi.org/10.1101/449884. The copyright holder for this preprint (which was not peer-reviewed) is the author/funder, who has granted bioRxiv a license to display the preprint in perpetuity. All rights reserved. No reuse allowed without permission.

batch of cell preparation (shown with a dotted line at 1). N=13 independent cell preparations. Data shown as mean ± SEM. One-sample t-test with Bonferroni correction; * p<0.05, ** p<0.01, *** p<0.001, ****p<0.0001.

FIGURE 4. LPS suppression of *Trem2* expression in primary microglia results in little effect of *Trem2* knockdown on LPS-induced gene expression. (a) The effect of LPS on *Trem2* expression with and without *Trem2* knockdown. Gene expression levels were normalized to *Rps28* and calculated as fold change relative to the negative control without LPS treatment in each individual culture preparation. (b) *Tnf* and *Il1b* expression, as examples of pro-inflammatory genes, were greatly up-regulated in primary microglia after LPS application. There was no significant difference between *Trem2* knockdown and negative controls. (c) ELISA analysis of the microglial supernatants showed that the secreted TNF-alpha levels in the medium were not significantly affected by *Trem2* knockdown. (d) Expression levels (RT-qPCR) of *C1qa, Cd68, Csf1r, Igf1, Pik3cg* and *Spi1* under the LPS-stimulated conditions in *Trem2*-knockdown microglia compared to negative controls. N=3-6 (RT-qPCR) and 4 (ELISA) independent microglial preparations. Data shown as mean ± SEM. Two-way ANOVA with significant main effect of LPS incubation time and *Trem2* knockdown indicated as horizontal and vertical lines respectively. The only significant interactions between LPS treatment and *Trem2* knockdown were in *Trem2* expression (panel a) and *Igf1* expression (panel d), and so Sidak's *post hoc* tests were performed to test pairwise significance between the negative siRNA control and *Trem2* knockdown. * p<0.05, ** p<0.01, *** p<0.001, **** p<0.0001.

FIGURE 5. *Trem2* knockdown impairs the IL4-induced anti-inflammatory response of primary microglia. (a) *Trem2* gene expression was not significantly influenced by IL4 stimulation. (b) *Arg1* and *Tgfb1* expression, as markers of the anti-inflammatory response, showed significant up-regulation with time after IL4 application. Particularly, *Trem2* knockdown greatly decreased IL4-induced *Arg1* expression compared to negative controls. (c) Expression of the pro-inflammatory genes *Tnf* and *Il1b* were inhibited with time after IL4 application. *Trem2* knockdown resulted in significantly

bioRxiv preprint first posted online Oct. 22, 2018; doi: http://dx.doi.org/10.1101/449884. The copyright holder for this preprint (which was not peer-reviewed) is the author/funder, who has granted bioRxiv a license to display the preprint in perpetuity. All rights reserved. No reuse allowed without permission.

decreased *Tnf* expression, though it did not change the effect of IL4. Gene expression levels were normalized to *Rps28* and calculated as fold change relative to the negative control without IL4 treatment in each individual culture preparation. N=7-9 independent experiments. Data shown as mean ± SEM. Two-way ANOVA with significant main effect of IL4 incubation time and *Trem2* knockdown indicated as horizontal and vertical lines respectively. A significant interaction between IL4 treatment and *Trem2* knockdown was seen only in *Arg1* expression (panel b), and so Sidak's *post hoc* tests were performed to test pairwise significance between the negative siRNA control and *Trem2* knockdown. * p<0.05, ** p<0.01, *** p<0.001, **** p<0.0001.

FIGURE 6. Effects of *Trem2* knockdown on gene expression changes in primary microglia with IL4 treatment. Gene expression levels were normalized to *Rps28* and calculated as fold change relative to the negative control without IL4 treatment in each individual culture preparation. N=7-9 independent experiments. Data shown as mean ± SEM. Two-way ANOVA; significant main effects of IL4 treatment time and *Trem2*-knockdown indicated by horizontal and vertical lines respectively, no significant interactions were seen between IL4 treatment and *Trem2* knockdown. * p<0.05, ** p<0.01, *** p<0.001, **** p<0.0001.

FIGURE 7. *Trem2* knockdown resulted in significantly decreased total STAT6 levels and AKT phosphorylation in primary microglia *in vitro*. (a-b) Total and phosphorylated STAT6 protein levels in primary microglia treated with IL4 and *Trem2* siRNA were analyzed with western blot. N=4 independent experiments. (c) *Stat6* gene expression levels in primary microglia, assessed by RT-qPCR (n=3 independent experiments). (d-e) Total and phosphorylated (at Thr308 and Ser473) AKT protein levels analyzed by western blot. N=4 independent experiments. Protein levels were normalized to beta-actin and gene expression was normalized to *Rps28*. Fold change was calculated relative to the negative control without IL4 treatment in each individual culture preparation. Note that phosphorylated STAT6 was not detectable under control conditions and so under IL4 conditions the effect of *Trem2* knockdown was calculated as fold change relative to control cells. Data shown as mean ±

bioRxiv preprint first posted online Oct. 22, 2018; doi: http://dx.doi.org/10.1101/449884. The copyright holder for this preprint (which was not peer-reviewed) is the author/funder, who has granted bioRxiv a license to display the preprint in perpetuity. All rights reserved. No reuse allowed without permission.

SEM. With the exception of phosphorylated STAT6, data were analyzed by two-way ANOVA; significant main effects of IL4 treatment and *Trem2*-knockdown indicated by horizontal and vertical lines respectively, no significant interactions were seen between IL4 treatment and *Trem2* knockdown. Phosphorylated STAT6 was analyzed by a one-sample t-test. * p<0.05, ** p<0.01, *** p<0.001, **** p<0.0001.

FIGURE 8. *Trem2* R47H knock-in mice (4 months old) showed significant down-regulation of *Trem2* expression, and decreased microglia density and CD68 levels in the hippocampus. (a) Gene expression in hippocampal homogenates from homozygous (HO) and heterozygous (HE) *Trem2* R47H KI mice relative to *Rps28* and then expressed relative to WT within the batch. N=6-7 mice per group. Data shown as mean ± SEM. One-way ANOVA showed a significant main effect of genotype for *Trem2* expression only, and so Sidak's *post hoc* tests were used to test pairwise significance between the three genotypes. * p<0.05, ** p<0.01, *** p<0.001. (b) Representative images showing AIF1 and CD68 immuno-staining of microglia with DAPI in the hippocampal CA1 regions from WT and HO-*Trem2* R47H KI mice. The layers from left are SO (*stratum oriens*), SP (*stratum pyramidale*), SR (*stratum radiatum)*, and SLM (*stratum lacunosum-moleculare*). Scale bar: 100 μm. (c) Left panel: total microglia density in all four CA1 layers was decreased in HO-*Trem2* R47H KI mice. Middle panel: density of CD68 positive microglia decreased in HO-*Trem2* R47H KI mice. Right panel: proportion of CD68 positive microglia was significantly lower in HO-*Trem2* R47H KI mice. N=5-6 mice per group. Data shown as mean ± SEM. Two-way ANOVA with significant main effect of *Trem2* genotype indicated with vertical lines, no significant interactions were seen between hippocampal layer and *Trem2* genotype. * p<0.05, ** p<0.01, *** p<0.001, **** p<0.0001.

FIGURE 9. Primary microglia from *Trem2* R47H knock-in mice show decreased *Trem2* expression, and changes to canonical markers in response to IL4 and LPS. (a) Expression of *Trem2*. (b) Expression of pro-inflammatory markers, *Tnf* and *Il1b.* (c) Expression of anti-inflammatory markers, *Tgf1b* and *Arg1*. Gene expression was normalized to *Rps28*. Dotted

bioRxiv preprint first posted online Oct. 22, 2018; doi: http://dx.doi.org/10.1101/449884. The copyright holder for this preprint (which was not peer-reviewed) is the author/funder, who has granted bioRxiv a license to display the preprint in perpetuity. All rights reserved. No reuse allowed without permission.

boxes show fold changes relative to untreated microglia. N=14-15 mice per genotype, except for genes *Il1b* and *Tgfb1,* where N=8-10 mice. Data shown as mean ± SEM. Two-way ANOVA with Bonferroni correction (for all genes except *Arg1*) were undertaken separately for IL4 and LPS using the same control data. Significant main effect of treatment (IL4 or LPS) and genotype indicated as horizontal and vertical lines respectively. A significant interaction between treatment and genotype was seen for only *Trem2* and *Tnf* expression, and so Sidak's *post hoc* tests were performed to test pairwise significance between the three genotypes within a treatment group, marked above individual groups for *Tnf*. For *Trem2* the interaction reflects a lack of effect of genotype in the LPS treated microglia. *Arg1* was analyzed by one-way ANOVA ($p = 0.002$) followed by Sidak's multiple comparisons to test pairwise significance between the three genotypes. * $p<0.05$, ** $p<0.01$, *** $p<0.001$, **** $p<0.0001$.

FIGURE 10. Altered gene expression profile in primary microglia from *Trem2* R47H knock-in mice. Expression of *Aif1, Csf1r, Plcg2, Igf1, Cd68* and *C1qa.* Gene expression was normalized to *Rps28*. N=14-15 mice per genotype (except for genes *Igf1*, *Cd68* and *C1qa* where N=8-10 mice). Data shown as mean ± SEM. Two-way ANOVA with Bonferroni correction (for all genes except *Arg1*) were undertaken separately for IL4 and LPS using the same control data. Significant main effect of treatment (IL4 or LPS) and genotype indicated as horizontal and vertical lines respectively. A significant interaction between treatment and genotype was seen for only *Igf1* and *C1qa* expression, and so Sidak's *post hoc* tests were performed to test pairwise significance between the three genotypes within a treatment group reflecting a lack of effect of genotype in the LPS treated microglia. * $p<0.05$, ** $p<0.01$, *** $p<0.001$, **** $p<0.0001$.

FIGURE 11. Proposed model of the involvement of TREM2 in IL4-induced anti-inflammatory response. LPS induces pro-inflammatory activation of microglia, which is accompanied by down-regulated *Trem2* expression, and so microglia with reduced TREM2 activity can undergo normal, or even enhanced, pro-inflammatory activation. Under non-stimulated

bioRxiv preprint first posted online Oct. 22, 2018; doi: http://dx.doi.org/10.1101/449884. The copyright holder for this preprint (which was not peer-reviewed) is the author/funder, who has granted bioRxiv a license to display the preprint in perpetuity. All rights reserved. No reuse allowed without permission.

conditions, a number of microglial genes are down-regulated when TREM2 activity is decreased, such as *Csf1r* expression, which may reduce the survival of microglia. However, IL4 induces an anti-inflammatory phenotype of microglia. As our data suggest, TREM2 signaling is involved in maintenance of microglial STAT6 levels, which in the IL4 pathway is phosphorylated and translocates to the nucleus and functions as a key transcription factor for IL4-induced gene expression changes, such as for *Arg1*. Thus, *Trem2* deficiency results in decreased STAT6 levels in the microglial, which leads to an impairment of IL4-induced signaling. TREM2 also regulates the levels of a number of genes that are up-regulated by IL4 (and suppressed by LPS), such as *Igf1* and *C1qa*.

Figure 1

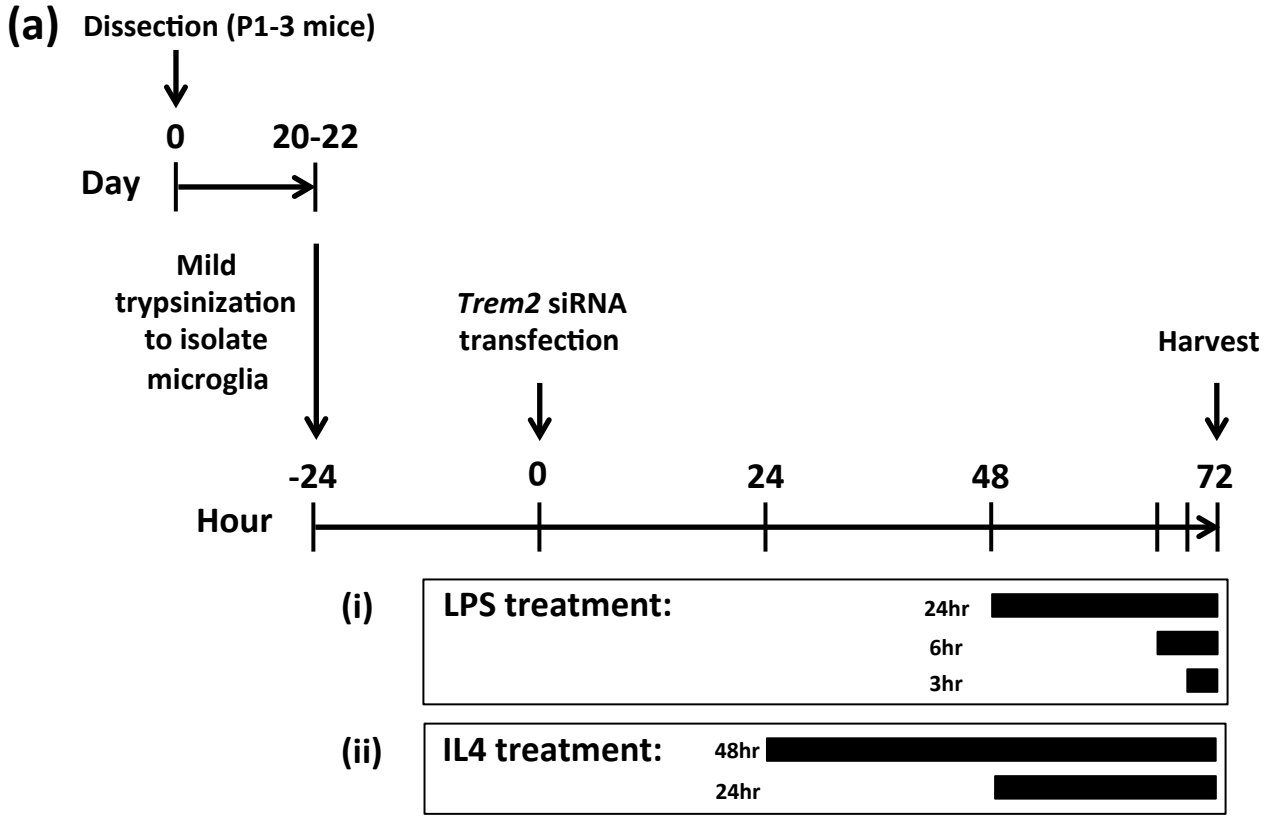
(a)
Dissection (P1-3 mice)
0
20-22
Day
Mild trypsinization to isolate microglia
Trem2 siRNA transfection
Harvest
-24
0
24
48
72
Hour
(i)
LPS treatment:
24hr
6hr
3hr
(ii)
IL4 treatment:
48hr
24hr

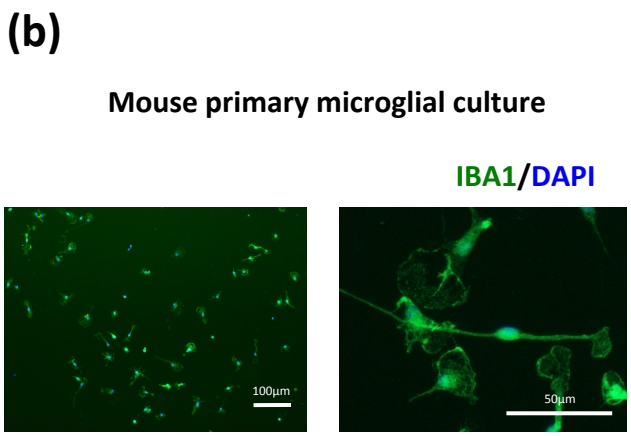
(b)
Mouse primary microglial culture
IBA1/DAPI
100μm
50μm

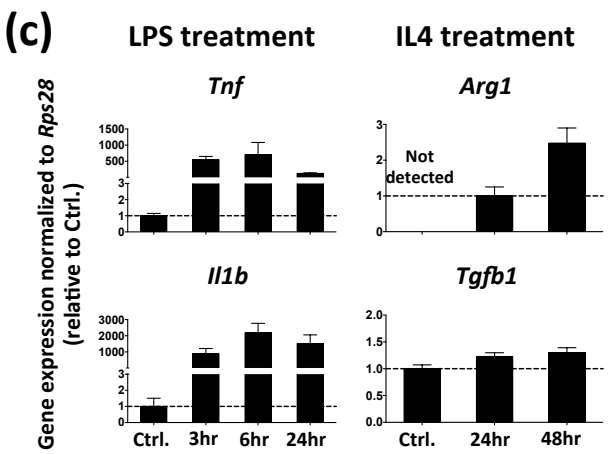
(c)
LPS treatment
IL4 treatment
Tnf
Arg1
Not detected
Il1b
Tgfb1
Gene expression normalized to Rps28 (relative to Ctrl.)
Ctrl.
3hr
6hr
24hr
Ctrl.
24hr
48hr

Figure 2

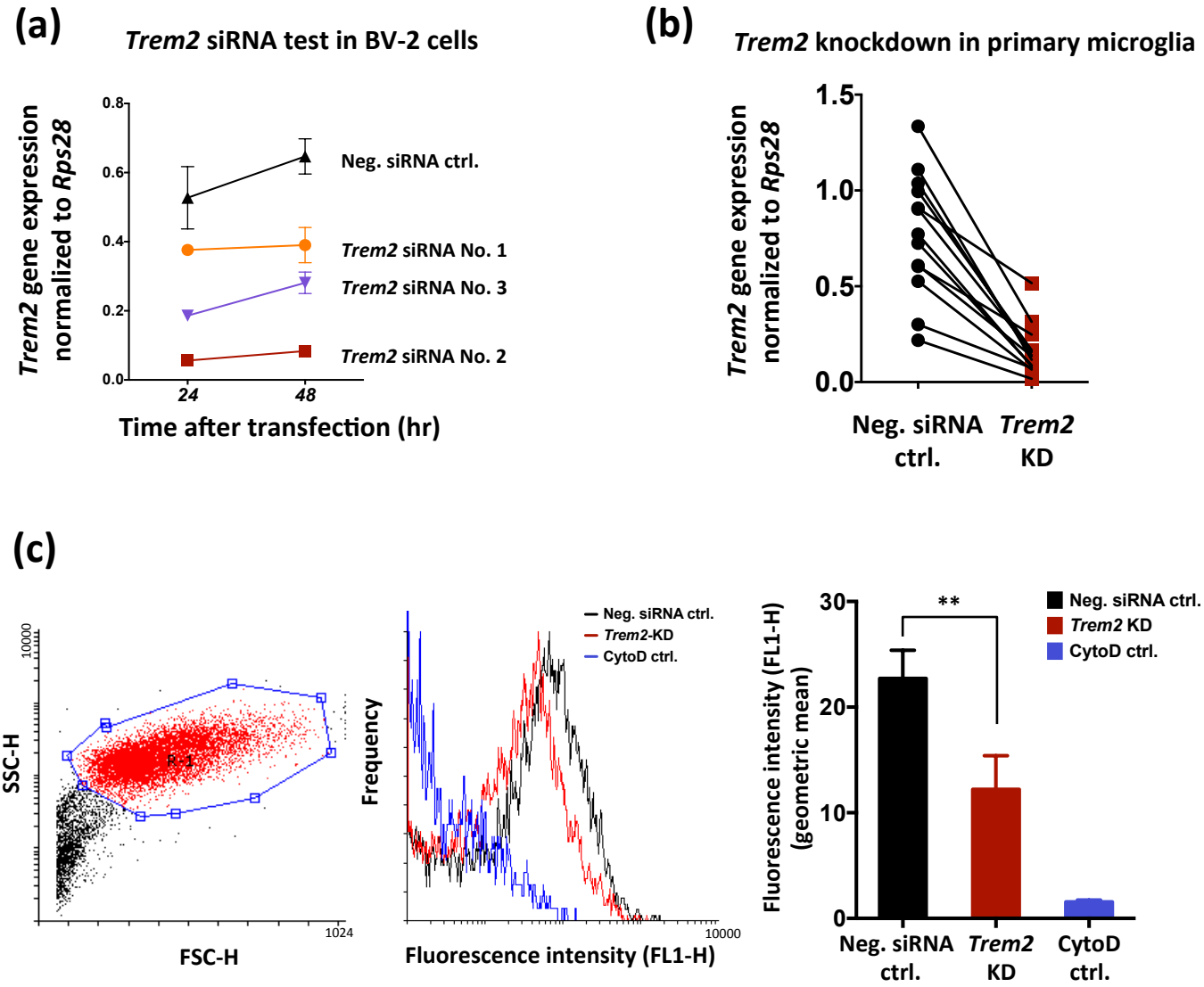
(a)
Trem2 siRNA test in BV-2 cells
Trem2 gene expression normalized to *Rps28*
0.8
0.6
0.4
0.2
0.0
Neg. siRNA ctrl.
Trem2 siRNA No. 1
Trem2 siRNA No. 3
Trem2 siRNA No. 2
24
48
Time after transfection (hr)
(b)
Trem2 knockdown in primary microglia
Trem2 gene expression normalized to *Rps28*
1.5
1.0
0.5
0.0
Neg. siRNA ctrl.
Trem2 KD
(c)
SSC-H
10000
1024
FSC-H
Frequency
Neg. siRNA ctrl.
Trem2-KD
CytoD ctrl.
10000
Fluorescence intensity (FL1-H)
Fluorescence intensity (FL1-H) (geometric mean)
30
20
10
0
**
Neg. siRNA ctrl.
Trem2 KD
CytoD ctrl.

Figure 3

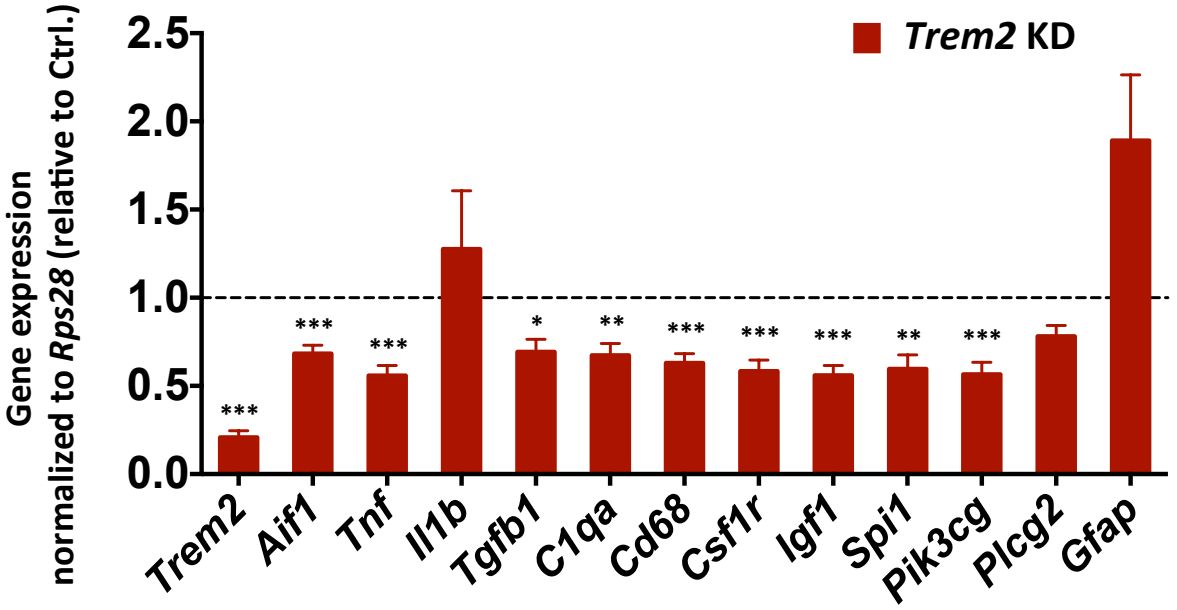
Trem2 KD
Gene expression normalized to Rps28 (relative to Ctrl.)
2.5
2.0
1.5
1.0
0.5
0.0
***
***
***
*
**
***
***
***
**
***
Trem2
Aif1
Tnf
Il1b
Tgfb1
C1qa
Cd68
Csf1r
Igf1
Spi1
Pik3cg
Plcg2
Gfap

Figure 4

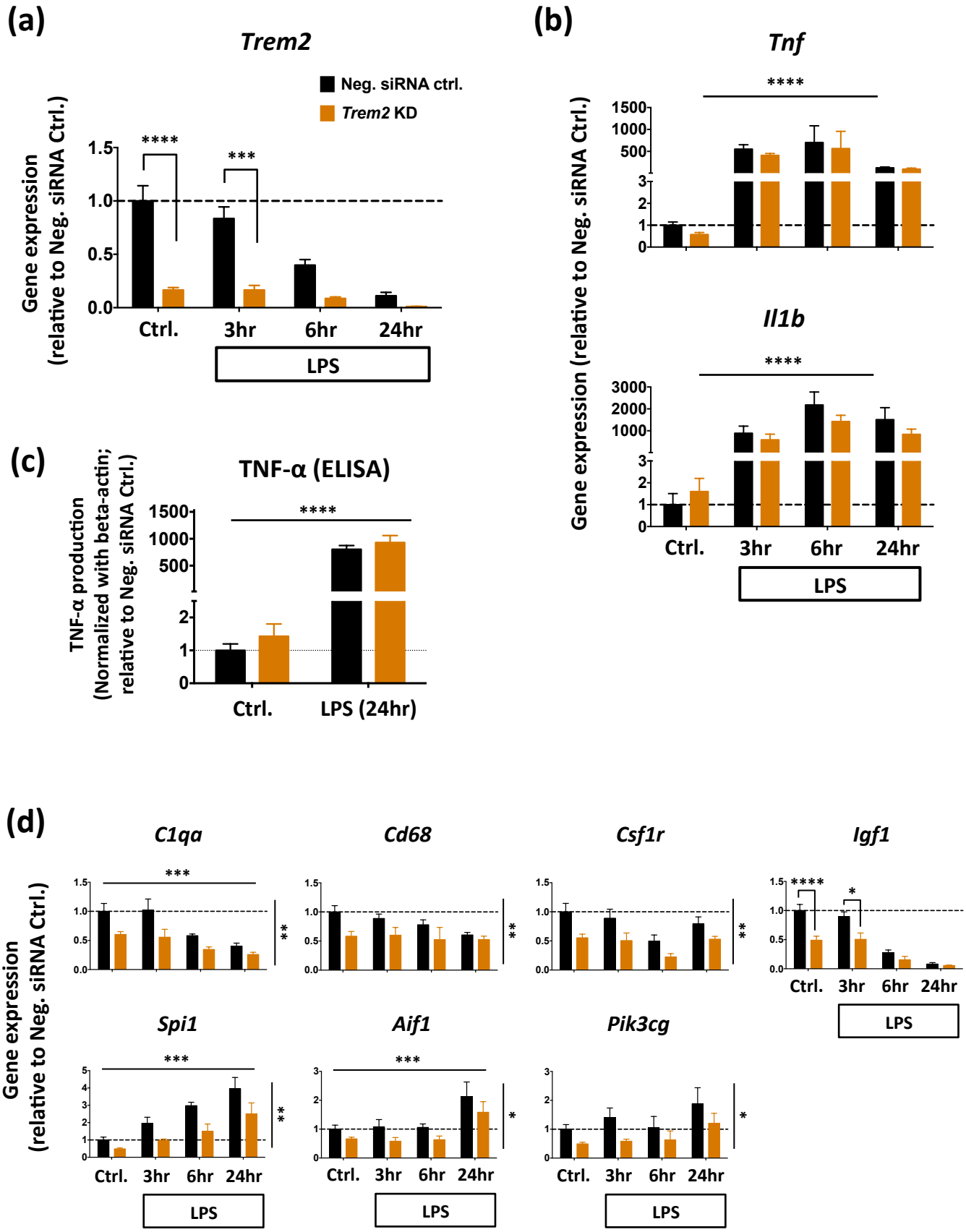
(a)
Trem2
Neg. siRNA ctrl.
Trem2 KD
Gene expression (relative to Neg. siRNA Ctrl.)
****
***
Ctrl.
3hr
6hr
24hr
LPS
(b)
Tnf
Il1b
Gene expression (relative to Neg. siRNA Ctrl.)
****
Ctrl.
3hr
6hr
24hr
LPS
(c)
TNF-α (ELISA)
TNF-α production (Normalized with beta-actin; relative to Neg. siRNA Ctrl.)
****
Ctrl.
LPS (24hr)
(d)
C1qa
Cd68
Csf1r
Igf1
Spi1
Aif1
Pik3cg
Gene expression (relative to Neg. siRNA Ctrl.)
Ctrl.
3hr
6hr
24hr
LPS

Figure 5

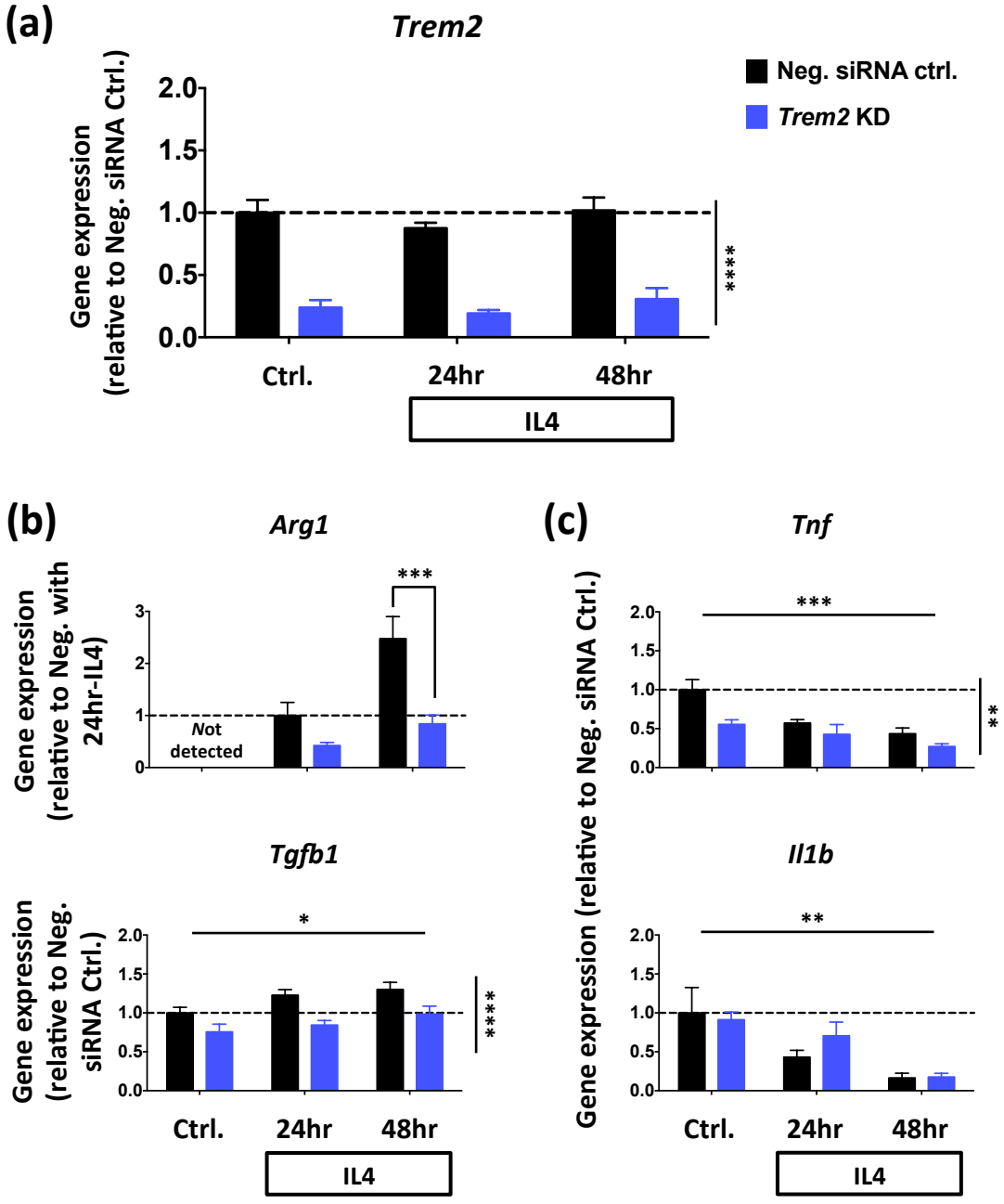
(a)
Trem2
Neg. siRNA ctrl.
Trem2 KD
Gene expression (relative to Neg. siRNA Ctrl.)
2.0
1.5
1.0
0.5
0.0
****
Ctrl.
24hr
48hr
IL4
(b)
Arg1
Gene expression (relative to Neg. with 24hr-IL4)
***
Not detected
Tgfb1
Gene expression (relative to Neg. siRNA Ctrl.)
*
****
(c)
Tnf
Gene expression (relative to Neg. siRNA Ctrl.)
***
**
Il1b
**

Figure 6

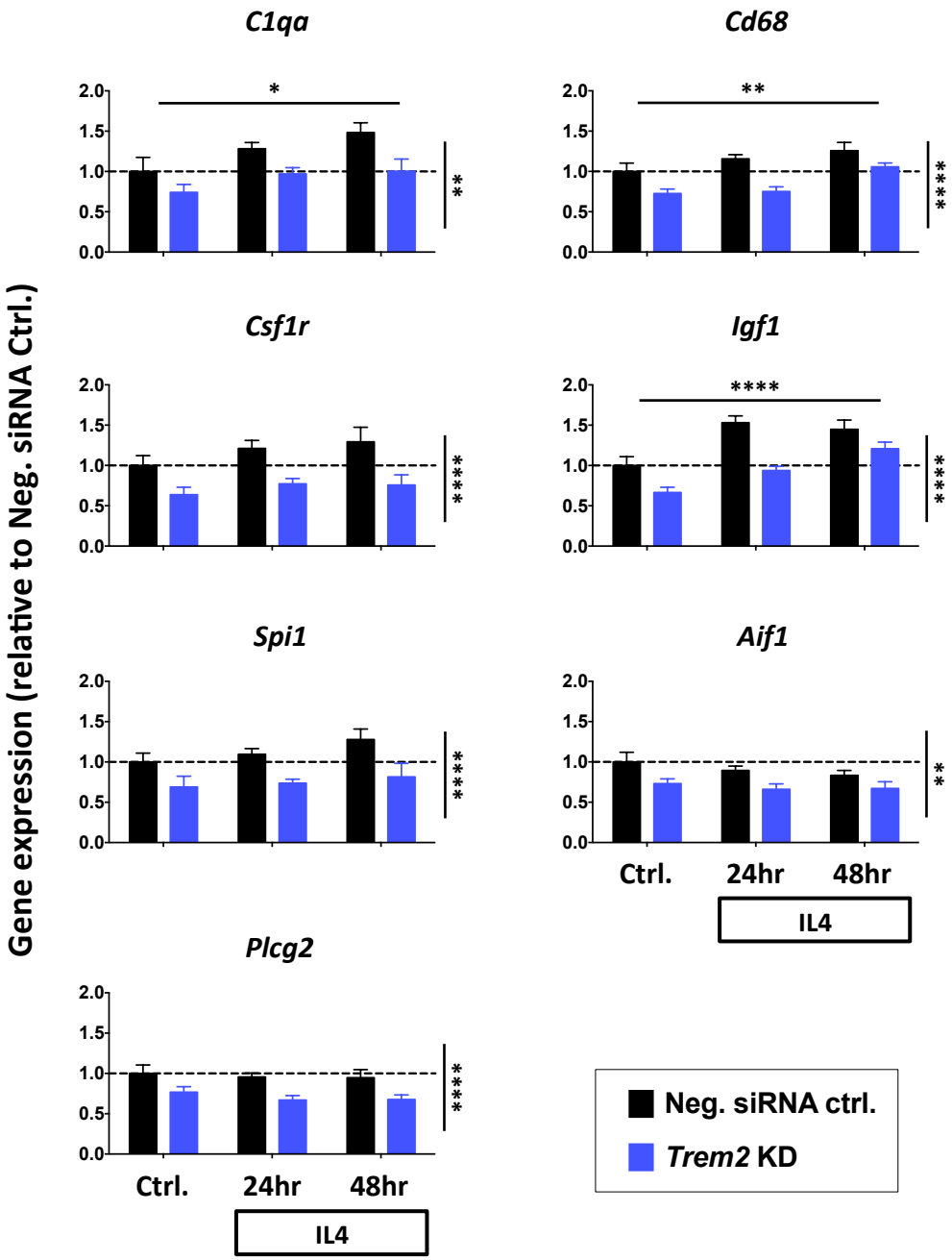
C1qa
Cd68
Csf1r
Igf1
Spi1
Aif1
Plcg2
Gene expression (relative to Neg. siRNA Ctrl.)
2.0
1.5
1.0
0.5
0.0
*
**
****
Ctrl.
24hr
48hr
IL4
Neg. siRNA ctrl.
Trem2 KD

Figure 7

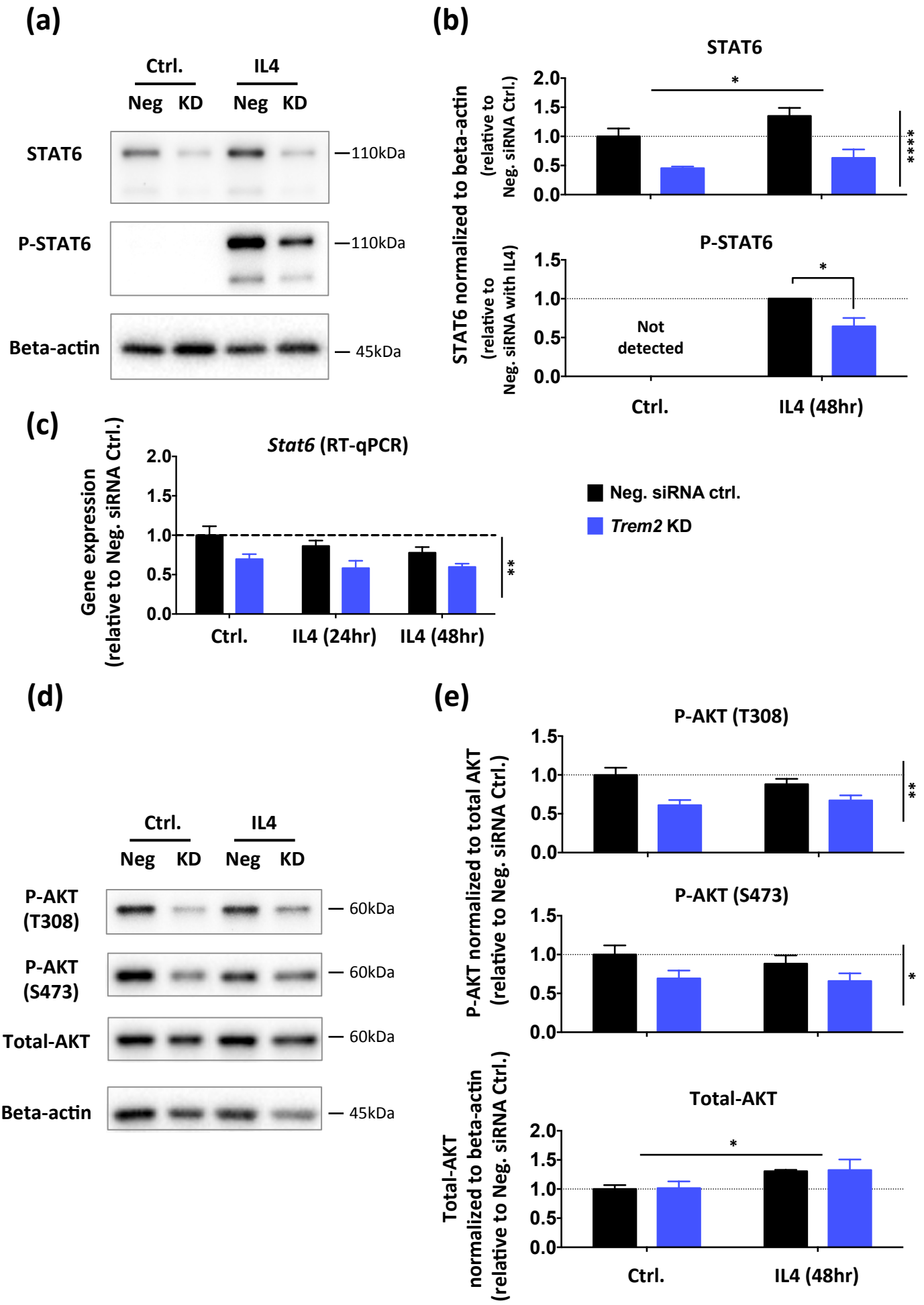
(a)
Ctrl.
IL4
Neg
KD
Neg
KD
STAT6
—110kDa
P-STAT6
—110kDa
Beta-actin
— 45kDa
(b)
STAT6
STAT6 normalized to beta-actin (relative to Neg. siRNA Ctrl.)
2.0
1.5
1.0
0.5
0.0
*
****
P-STAT6
STAT6 normalized to beta-actin (relative to Neg. siRNA with IL4)
1.5
1.0
0.5
0.0
*
Not detected
Ctrl.
IL4 (48hr)
(c)
Stat6 (RT-qPCR)
Gene expression (relative to Neg. siRNA Ctrl.)
2.0
1.5
1.0
0.5
0.0
**
Ctrl.
IL4 (24hr)
IL4 (48hr)
Neg. siRNA ctrl.
Trem2 KD
(d)
Ctrl.
IL4
Neg
KD
Neg
KD
P-AKT (T308)
— 60kDa
P-AKT (S473)
— 60kDa
Total-AKT
— 60kDa
Beta-actin
— 45kDa
(e)
P-AKT (T308)
P-AKT normalized to total AKT (relative to Neg. siRNA Ctrl.)
1.5
1.0
0.5
0.0
**
P-AKT (S473)
1.5
1.0
0.5
0.0
*
Total-AKT
Total-AKT normalized to beta-actin (relative to Neg. siRNA Ctrl.)
2.0
1.5
1.0
0.5
0.0
*
Ctrl.
IL4 (48hr)

Figure 8

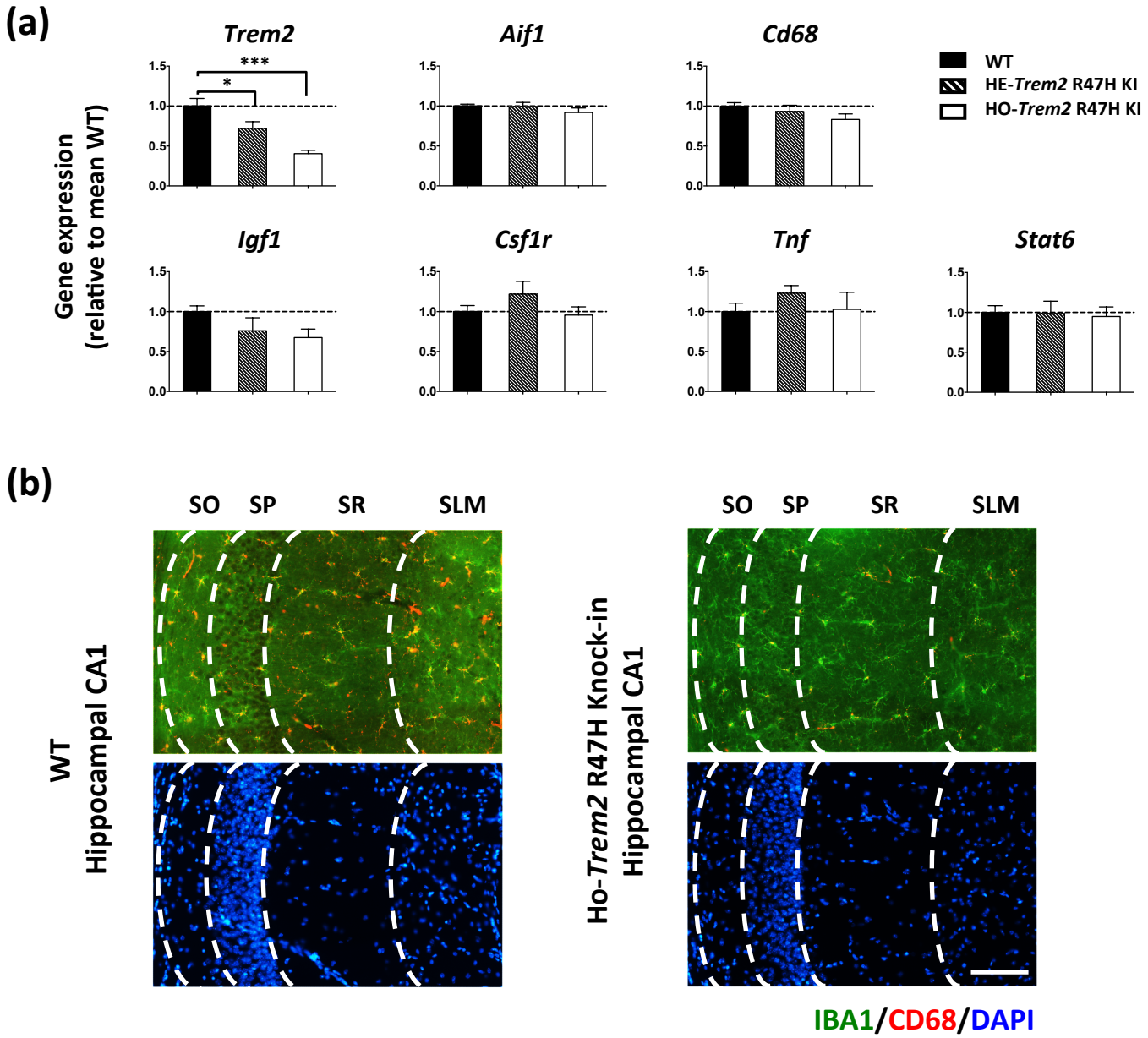
(a)
Trem2
Aif1
Cd68
Igf1
Csf1r
Tnf
Stat6
Gene expression (relative to mean WT)
WT
HE-Trem2 R47H KI
HO-Trem2 R47H KI
(b)
SO SP SR SLM
WT Hippocampal CA1
Ho-Trem2 R47H Knock-in Hippocampal CA1
IBA1/CD68/DAPI
(c)
Total Microglia
CD68+ Microglia
Cell Counts (per mm²)
CD68+/Total Microglia ratio
SO SP SR SLM

Figure 9

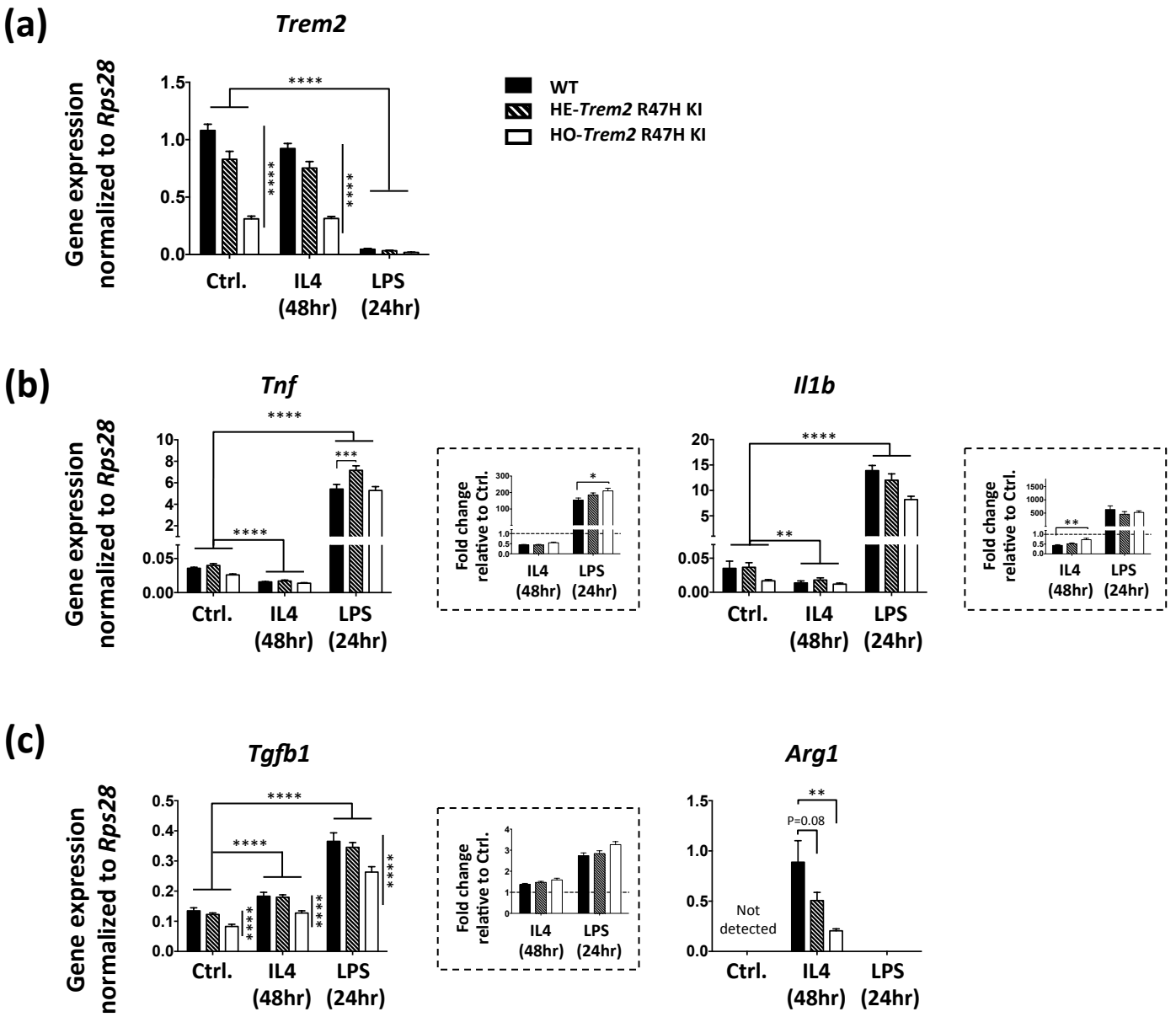
(a)
Trem2
Gene expression normalized to Rps28
WT
HE-Trem2 R47H KI
HO-Trem2 R47H KI
Ctrl.
IL4 (48hr)
LPS (24hr)
(b)
Tnf
Il1b
Fold change relative to Ctrl.
(c)
Tgfb1
Arg1
Not detected
P=0.08

Figure 10

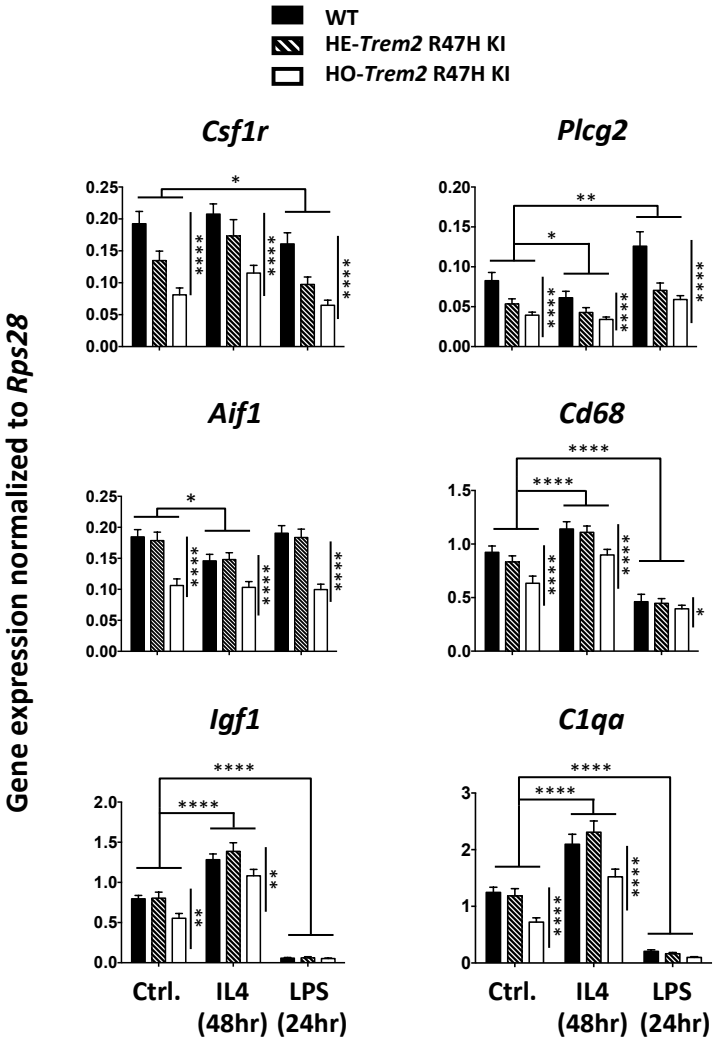
WT
HE-Trem2 R47H KI
HO-Trem2 R47H KI
Csf1r
Plcg2
Aif1
Cd68
Igf1
C1qa
Gene expression normalized to Rps28
Ctrl.
IL4 (48hr)
LPS (24hr)

Figure 11

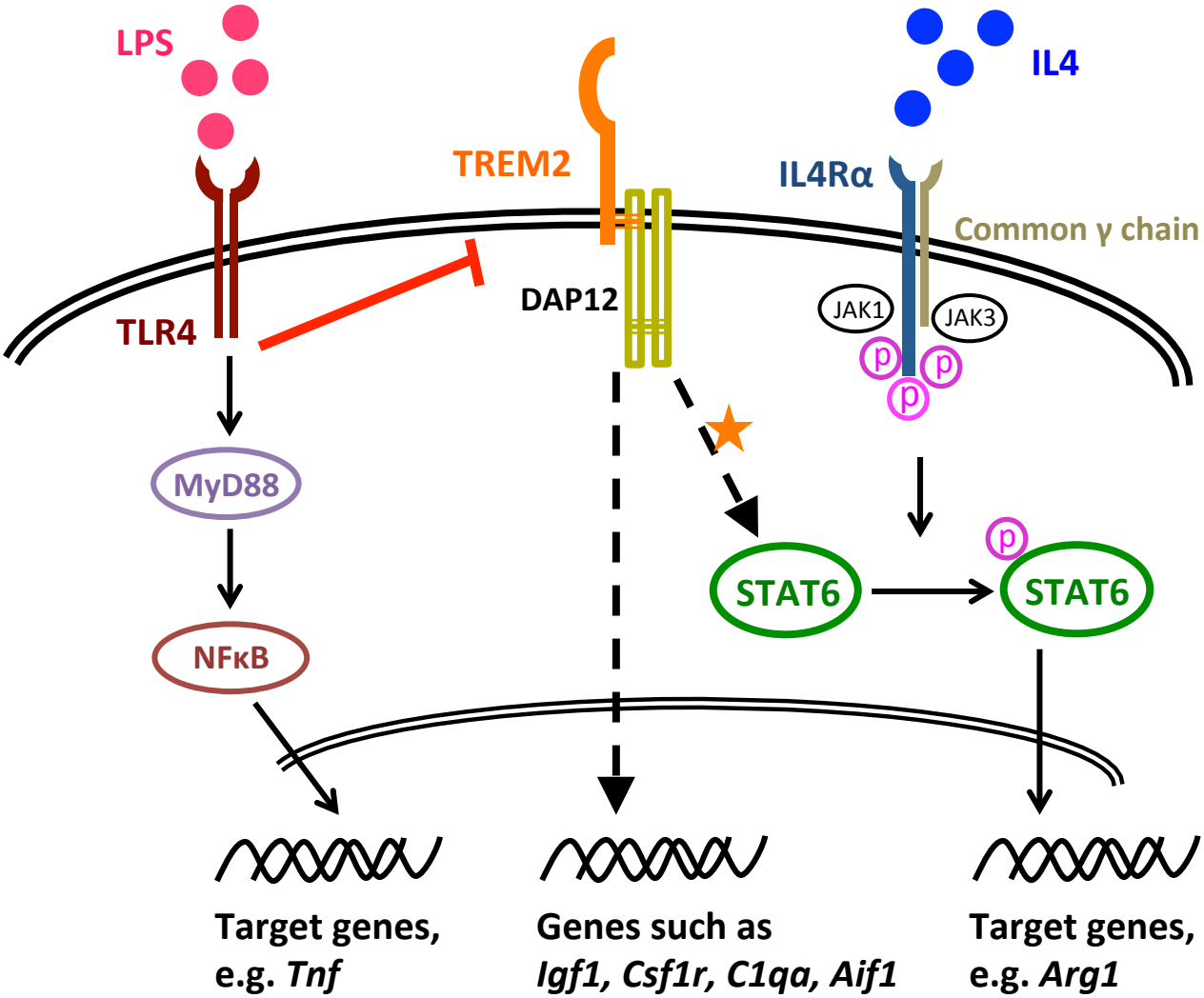
LPS
TREM2
IL4
IL4Rα
Common γ chain
DAP12
TLR4
JAK1
JAK3
p
p
p
MyD88
NFκB
STAT6
p
STAT6
Target genes,
e.g. Tnf
Genes such as
Igf1, Csf1r, C1qa, Aif1
Target genes,
e.g. Arg1